Structural, functional, and bioinformatics studies reveal a new snake venom homologue phospholipase A2 class

ARTICLE *in* PROTEINS STRUCTURE FUNCTION AND BIOINFORMATICS · JANUARY 2011

Impact Factor: 2.63 · DOI: 10.1002/prot.22858

PROTEINS
STRUCTURE ■ FUNCTION ■ BIOINFORMATICS

Structural, functional, and bioinformatics studies reveal a new snake venom homologue phospholipase A_2 class

Juliana I. dos Santos,[1#] Mariana Cintra-Francischinelli,[2#] Rafael J. Borges,[1] Carlos A. H. Fernandes,[1] Paola Pizzo,[2] Adélia C. O. Cintra,[3] Antonio S. K. Braz,[1] Andreimar M. Soares,[3] and Marcos R. M. Fontes[1*]

[1] Departamento de Física e Biofísica, Instituto de Biociências, UNESP – Univ Estadual Paulista, Botucatu-SP and Instituto Nacional de Ciência e Tecnologia em Toxinas, CNPq, Brazil

[2] Dipartimento di Scienze Biomediche, Università di Padova, Padova, Italy

[3] Departamento de Análises Clínicas, Toxicológicas e Bromatológicas, FCFRP, USP, Ribeirão Preto-SP, Brazil

ABSTRACT

Phospholipases A_2 (PLA_2s) are enzymes responsible for membrane disruption through Ca^{2+}-dependent hydrolysis of phospholipids. Lys49-PLA_2s are well-characterized homologue PLA_2s that do not show catalytic activity but can exert a pronounced local myotoxic effect. These homologue PLA_2s were first believed to present residual catalytic activity but experiments with a recombinant toxin show they are incapable of catalysis. Herein, we present a new homologue Asp49-PLA_2 (BthTX-II) that is also able to exert muscle damage. This toxin was isolated in 1992 and characterized as presenting very low catalytic activity. Interestingly, this myotoxic homologue Asp49-PLA_2 conserves all the residues responsible for Ca^{2+} coordination and of the catalytic network, features thought to be fundamental for PLA_2 enzymatic activity. Previous crystallographic studies of apo BthTX-II suggested this toxin could be catalytically inactive since a distortion in the calcium binding loop was observed. In this article, we show BthTX-II is not catalytic based on an *in vitro* cell viability assay and time-lapse experiments on C2C12 myotube cell cultures, X-ray crystallography and phylogenetic studies. Cell culture experiments show that BthTX-II is devoid of catalytic activity, as already observed for Lys49-PLA_2s. Crystallographic studies of the complex BthTX-II/Ca^{2+} show that the distortion of the calcium binding loop is still present and impairs ion coordination even though Ca^{2+} are found interacting with other regions of the protein. Phylogenetic studies demonstrate that BthTX-II is more phylogenetically related to Lys49-PLA_2s than to other Asp49-PLA_2s, thus allowing Crotalinae subfamily PLA_2s to be classified into two main branches: a catalytic and a myotoxic one.

Proteins 2010; 00:000–000.

Key words: phospholipase A_2; myotoxin; X-ray crystallography; phylogenetic analysis; myotube cell culture; calcium imaging.

INTRODUCTION

Phospholipases A_2 (PLA_2s) are small (~14kDa), stable, calcium-dependent, disulfide-rich enzymes that cleave membrane phospholipids at the *sn*-2 position, producing lysophospholipids and free fatty acids.[1] The released fatty acids can function as energy stores, second messengers[2,3] and precursors of eicosanoids, which are potent mediators of inflammation.[4,5] On the other hand, lysophospholipids are involved in cell signaling and phospholipid remodeling and are associated with membrane perturbation.[6,7] PLA_2s are structurally characterized by the conserved residues His48, Asp49, Tyr52, Tyr73, and Asp99 that constitute their catalytic network[8] (numbering system according to Renetseder *et al.*[9]). As a rule for typical PLA_2s (E.C. 3.1.1.4.), Ca^{2+} is considered an essential cofactor for their enzymatic activity,[10–12] in which Tyr28, Gly30, Gly32, and Asp49 are the residues usually involved in the ion coordination.[8,13,14]

These proteins are currently categorized into 15 classes[15] and are abundant and widespread in snake venoms.[16,17] Additionally, proteins that exhibit a natural amino acid mutation in position 49 and adopt a PLA_2 folding (e.g. Lys49-PLA_2s, Arg49-PLA_2s, Ser49-PLA_2s, Gln49-PLA_2s, and Asn49-PLA_2s) are also found in these venoms and are responsible for additional or other pharmacological properties such as neurotoxic, myotoxic, anticoagulant, bactericidal, hypotensive, and edema-inducing activities.[18–37]

Additional Supporting Information may be found in the online version of this article.

[#]The authors Juliana I. dos Santos and Mariana Cintra-Francischinelli contributed equally to this work.

A.S.K.B's current address is Univ Federal do ABC, CCNH, Santo André-SP, Brazil

*Correspondence to: M.R.M. Fontes, Departamento de Física e Biofísica, Instituto de Biociências, UNESP – Univ Estadual Paulista, Botucatu-SP and Instituto Nacional de Ciência e Tecnologia em Toxinas, CNPq, Brazil. E-mail: fontes@ibb.unesp.br
Received 18 May 2010; Revised 22 July 2010; Accepted 13 August 2010
Published online 23 August 2010 in Wiley Online Library (wileyonlinelibrary.com).
DOI: 10.1002/prot.22858

Their ability to exhibit such a diverse spectrum of activities is intriguing since PLA_2s share significant sequential and structural similarity and since these activities emerge from a single structural scaffold.[8]

The action mechanism(s) of myotoxins, which include the natural mutants Lys49-PLA_2s, Arg49-PLA_2s, Gln49-PLA_2s, Asn49-PLA_2s, Ser49-PLA_2s, and some Asp49-PLA_2s, are of great scientific interest since they are able to rapidly damage muscle fibers after snake bites and, like other proteins and peptides (e.g. metalloproteases), can provoke permanent tissue loss and disability.[38–42] Trials to efficiently neutralize these toxins have not yet achieved definitive results up to these days although many studies have been performed in recent years.[43]

Homologue Lys49-PLA_2s, the largest studied and best characterized subgroup among these proteins, are known to be myotoxic despite their lack of enzymatic activity.[34,44] This fact was first attributed to the natural amino acid substitution D49K presented by these PLA_2s[45] but later other peculiarities were also demonstrated to be involved in their loss of the catalytic activity.[44,46] Synthetic peptides and site-directed mutagenesis studies strongly suggest the C-terminal region of these proteins as being the domain responsible for this activity in Lys49-PLA_2s.[34,44,47–55] Replacement of Arg and Lys residues by Ala in the region 117–122 of BthTX-I resulted in a significant reduction of myotoxic activity.[47] Based on these and other studies, Lomonte and colleagues proposed that Lys49-PLA_2 action arises from the interaction of the C-terminal positive residues with membrane anionic phospholipids. Recently, after a review of many crystallographic structures of Lys49-PLA_2s, dos Santos *et al.* concluded that the residues Lys20, Lys115, and Arg118 probably constitute the myotoxic site of bothropic Lys49-PLA_2s.[56]

Other myotoxins, beyond this well-characterized subgroup, require deeper functional and structural studies. One of these subgroups includes the myotoxic Asp49-PLA_2s BthTX-II and PrTX-III, proteins that are able to induce muscle damage but present very low catalytic activity.[57–60] These toxins seem to be an exception among the classic Asp49-PLA_2s since they present reduced catalytic potency[18] even though they conserve the residues of the catalytic network.[59–62] BthTX-II, a basic Asp49-PLA_2 toxin from *B. jararacussu*, is also known for its edematogenic and hemolytic effects[57,58,63] and for its ability to induce platelet aggregation and secretion through multiple signal transduction pathways.[64] The residues between Thr112 and Pro121 from BthTX-II primary sequence are assumed to be responsible for its myotoxic activity.[30,59]

The maintenance of the calcium-binding-loop architecture is essential for the catalytic activity of snake venom PLA2s. Residues Tyr28, Gly30, and Gly32 from this region, together with Asp49, are responsible for Ca^{2+} coordination.[8,13,14] Recent structural studies on BthTX-II showed that the calcium binding loop of this protein is distorted when compared to classic Asp49-PLA_2s.[61] Rigden *et al.* had also observed this distortion when the PrTX-III crystallographic structure was solved.[62] Therefore, it was suggested that these toxins could be catalytically inactive.[61]

In this work we demonstrate that BthTX-II presents myotoxic activity but is not catalytic. This finding was achieved by experiments with C2C12 myotube cell culture and is supported by X-ray crystallography and phylogenetic studies. The Viperidae family evolution and the possible relationships between snake venom PLA_2s and some of their members that adopt a PLA_2 folding but do not present enzymatic activity are also discussed.

MATERIAL AND METHODS

BthTX-II purification and PLA_2 activity assay

BthTX-II was isolated from *Bothrops jararacussu* snake venom by gel filtration and ion-exchange chromatography as previously described.[57] Purity of the toxin was assessed in reduced conditions by polyacrylamide gel electrophoresis in the presence of sodium dodecylsulphate (SDS-PAGE) with Coomassie Blue staining. PLA_2 activity was measured with a $sPLA_2$ assay kit (Cayman Chemicals, Ann Arbor, MI), using the 1,2-dithio of diheptanoyl phosphatidylcholine analog, which serves as a substrate for most PLA_2s with exception of cytosolic PLA_2s. Upon hydrolysis of the thio-ester bond at the sn-2 position by PLA_2, free thiols were detected using DTNB (5,5-dithio-bis-(2-nitrobenzoic acid)).

Cellular studies

Cell culture

The murine skeletal muscle C2C12 cell line obtained from the American Type Culture Collection (CRL-1772, ATCC) was used as the toxin target. C2C12 cells were maintained at subconfluent levels in growth medium consisting of Dulbecco's modified Eagle medium (DMEM) (Gibco) supplemented with 10% foetal bovine serum (EuroClone). To induce differentiation (5–6 days), cells were grown to 80% confluence and then the medium was replaced with DMEM supplemented with 2% horse serum (Gibco) and changed every 24–48 h. For microscopy, cells were plated on coverslips (24 mm diameter) (10–20 $\times$ 10^4 cells/well) coated overnight with poly-L-lysine (Sigma) and then treated for 2 h with collagen (BD Biosciences).

Calcium measurements

Cells were loaded with fura-2 by incubation with 3 μM fura-2/AM at 37°C for about 30 min in modified

Krebs–Ringer Buffer (see below) containing 0.04% pluronic (Molecular Probes, Eugene, OR). To prevent fura-2 leakage and sequestration, 250 μM sulfinpyrazone was present throughout the loading procedure and $[Ca^{2+}]_c$ measurements. The coverslips were washed with a modified Krebs–Ringer Buffer (mKRB, 140mM NaCl, 2.8mM KCl, 2mM $MgCl_2$, 1mM $CaCl_2$, 10mM HEPES, 11mM glucose pH 7.4), mounted on a thermostated chamber (Medical System, NY) at 37°C, placed on the stage of an inverted microscope (Zeiss, Axiovert 100 TV) equipped for single cell fluorescence measurements and imaging analysis (TILL Photonics, Martinsried, Germany). Where indicated, a Ca^{2+}-free EGTA (200 μM)-containing medium was used. The sample was alternatively illuminated (t = 200 ms) by monochromatic light (at 340 and 380 nm wave lengths), every second for 10 min after toxin exposure, through a 40× oil immersion objective (NA = 1.30; Zeiss). The emitted fluorescence was passed through a dichroic beamsplitter (455DRPL), filtered at 505–530 nm (Omega Optical and Chroma Technologies, Brattleboro, VT) and captured by a cooled CCD camera (Imago, TILL Photonics). For presentation, the ratios (F340/F380) of different cells were off-line normalized to the resting value measured within the first minute of the experiment.

Cytotoxicity assay

Differentiated myotubes were grown in 96-well plates and then exposed to toxin for ten or thirty minutes; their viability was then measured with the MTS (3-(4,5-dimethylthiazol-2-yl-5-)3-carboxymethoxyphenyl-2-(4-sulfonphenyl)-2H-tetrazolium, inner salt) assay. The CellTiter 96 AQueous One Solution Cell Proliferation Assay (Promega) was used and instructions from the manufacturer were followed. Each cytotoxicity test was repeated 3–6 times. The percentage of cell death was expressed as the mean ± SEM. Student's t-test was used for statistical comparison of the data. A value of $P < 0.05$ was considered to indicate significance.

Crystallographic studies

Crystallization of BthTX-II in the presence of Ca^{2+}

Cocrystallization experiments were performed with lyophilized samples of BthTX-II[57] in the presence of calcium. The protein was dissolved in ultrapure water at a concentration of 12 mg mL^{-1}. A ratio of 30 ions for each protein molecule was considered for cocrystallization experiments. Crystals were obtained by the hanging drop vapor diffusion method[65] in the same crystallization condition under which the apo BthTX-II was crystallized: 20% (v/v) 2-propanol, 13% (w/v) polyethylene glycol 4000, and 0.05M sodium citrate pH 5.6.[61] Calcium chloride 0.01M was added in the crystallization drop as calcium ions source.

X-ray data collection, processing, structure determination, and refinement

X-ray diffraction data were collected using a wavelength of 1.427 Å at a synchrotron-radiation source (MX2 station - LNLS, Campinas, Brazil). Crystals were mounted in a nylon loop and flash-cooled in a nitrogen stream at 100 K without cryoprotectant. Data were processed using the HKL program package.[66]

The crystals were highly isomorphous with the crystals of apo BthTX-II[61]; therefore this structure (PDB code 2OQD) was used as starting model for crystallographic refinement. The model was improved, as judged by the free R-factor,[67] through rounds of crystallographic refinement using the REFMAC program,[68] and manual rebuilding was performed with the "Coot" program.[69] During the refinement 111 water molecules were added to the BthTX-II/ Ca^{2+} model. Due to the lack of electron density, side chains of the following residues were excluded: Arg43, Lys54, Lys69, Glu78, Ile82, Glu86, Lys114, Lys115, Asp122, Lys128, and Lys132 of monomer A; and Arg111 and Lys115 of monomer B.

The insertion of calcium ions in the crystallographic model was carefully analyzed and refined. The candidate regions for calcium placement were found by electron density inspection and using the function "find ligands" of the software Coot[69] using the difference map (F_{obs-} F_{calc}) with a signal of at least 3σ. The following prerequisites were used for their maintenance in the structure: (i) occupancy values higher than 0.7 after refinement (CNS program[70]); (ii) I/σ higher than 2.5 in the $2F_{obs-}F_{calc}$ map; (iii) preference for donor atoms of nitrogen, sulphur, and specially oxygen; (iv) coordination number and shape of coordination group (including presence of bidendate ligands).[71–73] Only interactions below 3.6 Å were considered, a value that includes primary and secondary coordination spheres.[71] Additionally, the possibility of water molecules in the same position was also investigated and discarded.

The refinement statistics for the final model are shown in Table I. The quality of the model was checked by the Procheck program.[74]

Comparative structural studies

Molecular comparison between the crystallographic structure of apo BthTX-II[61] (PDB id code 2OQD) and BthTX-II/Ca^{2+} was performed using the "O" program.[75] The same program was used to perform comparative analyses between BthTX-II and other Asp-PLA_2s and Lys49-PLA_2s which have X-ray crystallographic structures available in the Protein Data Bank (PDB—http://www.pdb.org). For all these purposes, only C^{α} coordinates were considered.

Analyses of the quaternary assemblies and interfacial contacts of the crystallographic models were performed using PISA program[76] available at the European Bioinformatics Institute server (http://www.ebi.ac.uk/msd-srv/prot_int/pistart.html). All the figures corresponding to

Table I
X-ray Data Collection and Refinement Statistics for BthTX-II/Ca^{2+}

Unit cell (Å)	a = 59.24
	b = 100.88
	c = 47.17
Space group	C2
Resolution (Å)	50.44–2.10 (2.20–2.10)[a]
Unique reflections	12718 (1625)[a]
Completeness	97.4 (99.4)[a]
R_{merge}[b] (%)	10.4 (51.00)[a]
Radiation source	Synchrotron (LNLS—MX2)
Data collection temperature (K)	100
I/σ (I)	10.79 (2.55)[a]
Redundancy	3.7 (3.5)[a]
Molecules in asymmetric unit	2
R_{cryst}[c] (%)	21.7
R_{free}[d] (%)	24.9
Mean B-factor (Å^2)[e]	
Overall	39.7
Protein	40.1
Calcium ions	59.6
Water molecules	55.1
Mean Occupancy—calcium ions	0.90
R.m.s. deviations from ideal values[e]	
Bond lengths (Å)	0.019
Bond angles (°)	1.68
Ramachandran plot[f]	
Residues in most favorable region (%)	89.2
Residues in additionally allowed regions (%)	10.8
Residues in generously/not allowed regions (%)	0

[a]Numbers in parenthesis are for the highest resolution shell.
[b]$R_{merge} = \Sigma_{hkl}(\Sigma_i(|I_{hkl,i} - \langle I_{hkl}\rangle|))/\Sigma_{hkl,i}\langle I_{hkl}\rangle$, where $I_{hkl,i}$ is the intensity of an individual measurement of the reflection with Miller indices *h*, *k*, and *l*, and $\langle I_{hkl}\rangle$ is the mean intensity of that reflection. Calculated for $I > -3\sigma$ *(I)*.
[c]$R_{cryst} = R_{hkl}(||Fobs_{hkl}| - |Fcalc_{hkl}||)/|Fobs_{hkl}|$, where $|Fobs_{hkl}|$ and $|Fcalc_{hkl}|$ are the observed and calculated structure factor amplitudes.
[d]R_{free} is equivalent to R_{cryst} but calculated with reflections (5%) omitted from the refinement process.
[e]Calculated with the program CNS[1].
[f]Calculated with the program PROCHECK[2].

oligomeric analyses were generated using the Pymol program.[77]

Dynamic light scattering

The dynamic light scattering (DLS) measurements were performed with lyophilized BthTX-II at 283 K, at a concentration of 3.5 mg mL^{-1} using the instrument DynaPro TITAN (Wyatt Technology). The protein was prepared with the same buffer used in the crystallization condition (100 mM sodium citrate pH 5.6). Data were measured one hundred times and results were analyzed with Dynamics v.6.10 software.

Phylogenetic studies

Identification of homologous sequences

Homologous sequences were obtained from the NCBI database (http://www.ncbi.nlm.nih.gov) using the BLASTP algorithm and the Bothropstoxin I sequence (GI: 265051) from *Bothrops jararacussu* as the query. The BLOSUM62 matrix was used for scoring alignments, with other algorithm parameters set as default. The minimum *e*-value presented by the selected sequences was 3.10^{-44}. The selected homologous proteins and their respective database identification codes are shown in Table V.

Sequence alignment and phylogenetic analysis

Alignment of the selected sequences was performed by AMAP program v. 2.0.[78] The final alignment was used to construct a phylogenetic tree by Bayesian inference utilizing MrBayes v. 3.1.1 software.[79] Two concurrent MCMC runs of 3,000,000 generations were used using four progressively heated chains, a temperature value of 0.2, tree sampling every 100 generations and a burn-in of 2500 trees. The phylogenetic tree was visualized using the Mesquite program version 2.72.[80] All the protein sequences used in the phylogenetic analysis and their respective identification codes are shown in Table V.

RESULTS AND DISCUSSION

Characterization of BthTX-II and its effects on C2C12 myotubes

BthTX-II is able to form a dimer in solution as observed in SDS-PAGE and dynamic light scattering experiments. DLS experiments performed with BthTX-II indicated a mean hydrodynamic radius (R_H) of 2.5 nm and a polydispersity of 10.7%. This R_H value corresponds to a molecular weight of ~27 kDa and is, thus, equivalent to a dimer. This finding is in agreement with previous studies[59,61] and demonstrates the natural tendency of *Bothrops* myotoxins to oligomerize.[30,61,62,81–88]

Measurement of BthTX-II ability to cleave phospholipids revealed that its activity was 0.097 ± 0.017 μmol/min/mg. This value is much lower than those presented by other Asp49-PLA_2s (e.g. 282.0 ± 24.6 μmol/min/mg for Mt-I, a myotoxic Asp49-PLA_2 from *B. asper*[89] but comparable with those produced by Lys49-PLA_2s[89] (0.028 ± 0.003 and 0.62 ± 0.42 μmol/min/mg, respectively, for Mt-II and BthTX-I[89]). This curious finding gives rise to an interesting question: is extracellular calcium necessary to enable BthTX-II toxin to exert its action?

To answer this question calcium imaging experiments, cell viability assay and time-lapse experiments were performed on C2C12 myotubes bathed in medium with or without extracellular calcium. BthTX-II caused a progressive degeneration of myotubes as can be observed by loss of their morphology, accumulation of aggregates in their cytosol, fragmentation and eventually disappearance of their sarcolemma (Fig. 1). BthTX-II was able to cause cellular damage also in the absence of extracellular calcium (Fig. 2), while control cells maintained their normal morphology (data not shown).

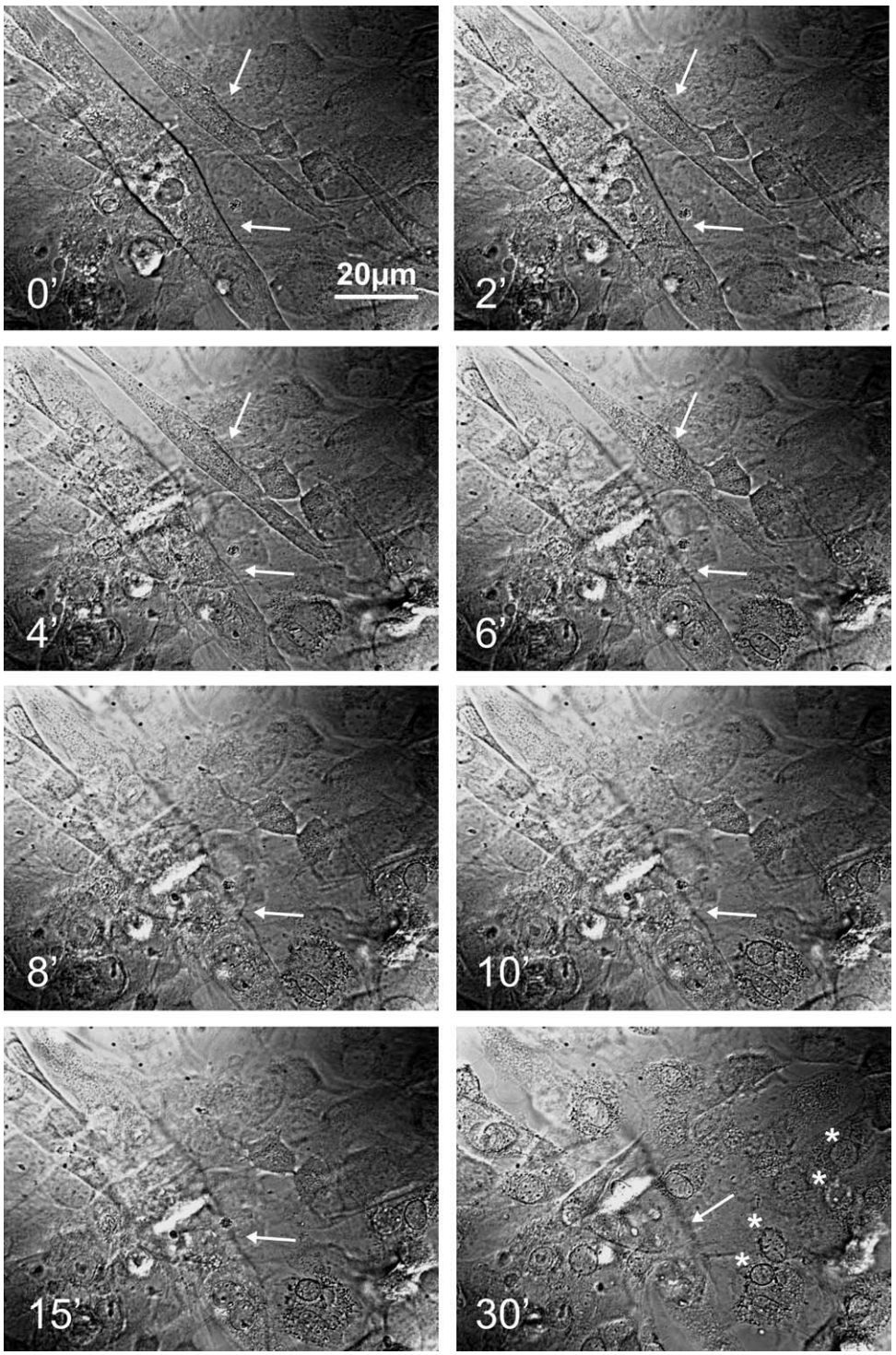

Figure 1

Time-lapse images show morphological changes induced by BthTX-II in C2C12 cells. Myotubes were treated with BthTX-II (50 μg/mL) for 30 min in Ca^{2+}-containing buffer and were observed in bright field. Arrows indicate myotubes, differentiated C2C12 cells. After 6 minutes it is possible to observe disruption of plasma membranes with loss of myotubes' morphology and at 30 minutes some damaged cells are observed as nuclei (asterisks).

Cytosolic calcium concentration, $[Ca^{2+}]_c$, measurements in differentiated C2C12 myotubes showed that BthTX-II caused a rapid increase in $[Ca^{2+}]_c$ followed by a second irregular rise characterized by slow waves [Fig. 3(A)]. In Ca^{2+}-free medium supplemented with EGTA, the first Ca^{2+} peak was still observed but the second

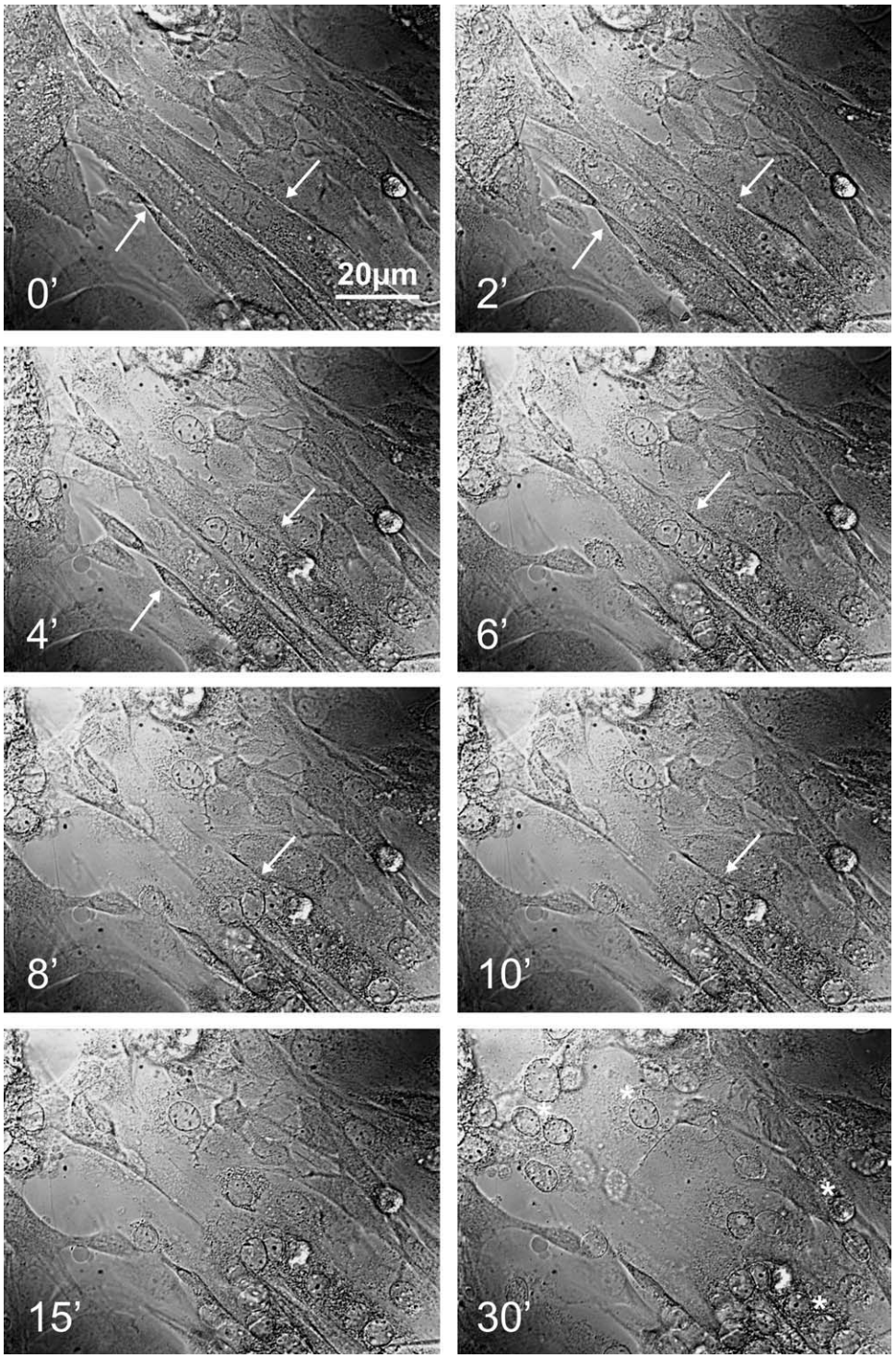

Figure 2

Time-lapse images show morphological changes induced by BthTX-II in C2C12 cells. Myotubes were treated with BthTX-II (50 µg/mL) for 30 min in Ca^{2+}-free medium supplemented with EGTA and observed in bright field. Arrows indicate myotubes, differentiated C2C12 cells. After 6 minutes it is possible to observe disruption of plasma membranes with loss of myotubess' morphology and at 30 minutes some damaged cells are observed as nuclei (asterisks).

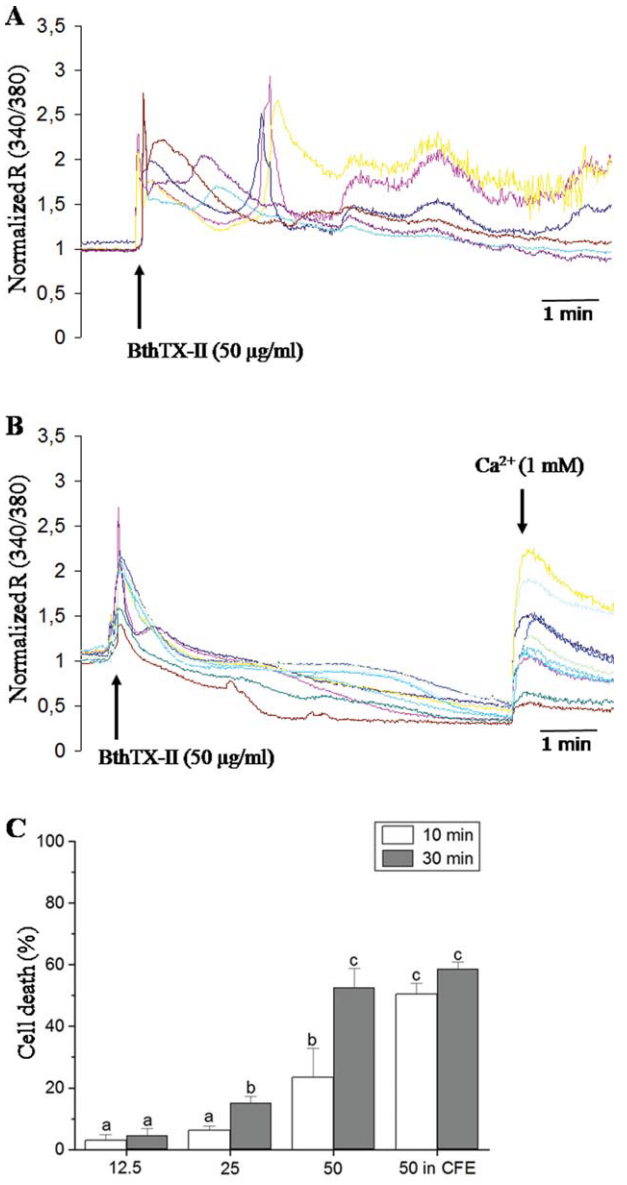

Figure 3

Effects of BthTX-II on $[Ca^{2+}]_c$ and viability of C2C12 myotubes. Panels A and B show intracellular calcium profiles in myotubes. The $[Ca^{2+}]_c$ was tracked as a change in the fura-2 fluorescence ratio (340/380 nm) in different cells after addition of BthTX-II (50 µg/mL) in Ca^{2+}-containing buffer (Panel A), or in Ca^{2+}-free EGTA-containing medium (Panel B). Owing to the elongated shape of myotubes, the individual traces refer to different cells or to different regions of the same cell. For presentation, the ratios were normalized to the resting value. Panel C shows percentages of cell death after treatment with different doses of BthTX-II for 10 (empty bars) or 30 minutes (gray bars). Bars represent mean values ± SEM estimated in three or more experiments performed in duplicates. Student's *t*-test was used for statistical comparison of the data. A value of $P < 0.05$ was considered to indicate significance. [Color figure can be viewed in the online issue, which is available at wileyonlinelibrary.com.]

irregular $[Ca^{2+}]_c$ rise was completely abolished [Fig. 3(B)], indicating the extracellular Ca^{2+} source of this second event, as also observed with other Lys49-PLA_2 and Asp49-PLA_2 toxins.[89] However, even under this condition, BthTX-II was able to alter the myotube plasma membrane permeability, since the addition of calcium to the cells [1 mM; arrow in Fig. 3(B)] caused a clear $[Ca^{2+}]_c$ rise, indicating a Ca^{2+} influx through the plasma membrane, differently from the controls where no $[Ca^{2+}]_c$ increase was observed (data not shown). In agreement with these findings, cell death of myotubes exposed to BthTX-II increased significantly in a time- and dose-dependent manner [Fig. 3(C)]. Using the same toxin concentration (50 µg/mL), the cytotoxic effect of BthTX-II was also observed in the absence of extracellular calcium and was actually moderately stronger than under physiological conditions at 10 min [Fig. 3(C)].

These results clearly show that BthTX-II is able to exert its function even in the absence of extracellular calcium, which is contrary to the notion that all Asp49-PLA_2s are enzymatically active and Ca^{2+}-dependent proteins.

Crystallographic structure of BthTX-II grown in the presence of calcium

Crystals of BthTX-II/Ca^{2+} were obtained under the same crystallization conditions in which the apo protein was crystallized[61] and diffracted X-rays to 2.10 Å resolution. Data-processing and refinement statistics are presented in Table I. The final model presents a final *R* value of 21.7% (R_{free} of 24.9%).

A dimer was found in the asymmetric unit of the crystal as indicated by the Mathews coefficient,[90] and in agreement with DLS and electrophoresis experiments. BthTX-II/Ca^{2+} crystal structure is isomorphous to the apo form of the protein and belongs to the C2 space group[61] (Table I). Examination of unit-cell packing showed two possible dimeric configurations for this structure, as already described by Côrrea *et al.*[61] The quaternary assembly chosen for apo BthTX-II in which the monomers are related by an approximated two–fold axis perpendicular to its β-wings was also used for BthTX-II/Ca^{2+} (Fig. 4). This dimeric configuration resembles the "conventional dimer" configuration adopted by Lys49-PLA_2s[46,56,91] and had already been observed by Rigden *et al.* when they solved the PrTX-III structure.[62]

Seven disulfide bridges were found in each monomer of the structure, conserving structural features of other class II PLA_2s, including the catalytic network constituted by His48, Tyr52, Tyr73, and Asp99[8,14] and the residues involved in Ca^{2+} coordination (Tyr28, Gly30, Gly32, and Asp49).[8,13,14] Even in the presence of a great amount of calcium ions, no Ca^{2+} was found in the calcium binding loop region. On the other hand, calcium ions were observed interacting with two equivalent regions in BthTX-II monomers (Fig. 1 – Supporting information). This finding may be related to the high concentration of calcium chloride used in the crystallization experiment

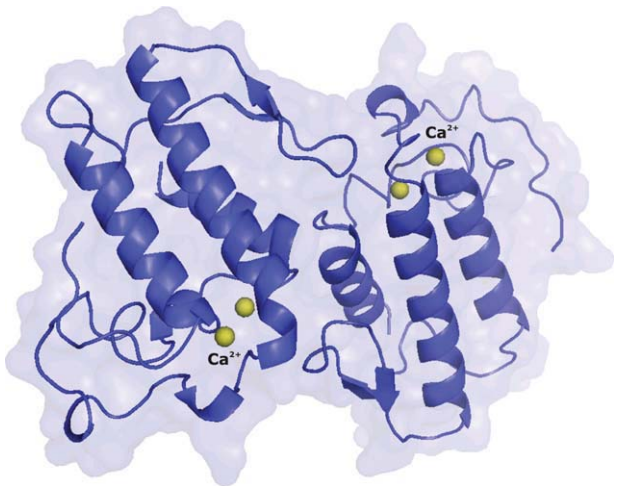

Figure 4

BthTX-II/Ca^{2+} crystallographic structure. Calcium ions are shown in yellow. [Color figure can be viewed in the online issue, which is available at wileyonlinelibrary.com.]

and probably have no biological significance. Additionally, the possibility of water molecules in the same positions was checked and discarded since their temperature factors and electronic density maps were in disagreement with other water molecules.

Comparison between apo BthTX-II and its complexed form

Superposition of apo BthTX-II and BthTX-II/Ca^{2+} dimeric forms resulted in C^{α} atom r.m.s. deviations of 0.39 and 0.55 Å for A and B monomers, respectively. Additionally, superposition of the two BthTX-II/Ca^{2+} monomers showed that they are similar (r.m.s.d. = 0.77 Å). The same occurred with the monomers of apo BthTX-II structure which showed an r.m.s.d. of 0.73 Å. The calcium binding loop of BthTX-II/Ca^{2+} structure is kept in the same orientation as the one observed for the apo form of the protein (Fig. 5). This observation explains why no Ca^{2+} was found interacting with this region since Côrrea *et al.* have reported that this loop presents a distorted conformation in the apo form of BthTX-II, a feature that impairs Ca^{2+} coordination.[61]

Comparison of apo and complexed BthTX-II structures indicated that some side chains present different rotameric configurations, despite the apparent absence of a relationship between these findings and the presence of calcium ions in some regions. These differences may be related to the different resolutions presented by the two structures (2.19 and 2.10 Å for apo and complexed forms, respectively). The region comprising the residues 77–81 from monomer B of BthTX-II/Ca^{2+} present a higher r.m.s.d. when compared to the same region of the apo form of BthtX-II (encircled in Fig. 5). Given the 10.5 Å distance between the calcium ion and the closest atom of BthTX-II/Ca^{2+} monomer B (oxygen from the main chain of Glu78), it is unlikely that calcium ion led to this distortion. No other significant differences were observed between apo and cocrystallized structures (Fig. 5), suggesting that calcium ions do not induce any alteration in the tertiary or even in the quaternary conformation of the protein under study.

Comparison between BthTX-II forms and other PLA_2s

In order to get insights that could explain why BthTX-II is not catalytic, comparative studies between the amino acid sequence of this protein and other classic and myotoxic Asp49-PLA_2s from the Crotalinae subfamily were performed showing that the residues of their catalytic network (e.g. His48, Asp49, Tyr52, and Asp99) and the ones responsible for calcium coordination (e.g. Tyr28, Gly30, and Gly32) are fully conserved.[46,59,60] Therefore, it was expected that any Asp49-PLA_2 would present catalytic activity. Since no clue was ascertained by only sequence alignment analyses, the X-ray crystallographic structures were superposed.

A three-dimensional analyses of the calcium binding loop region demonstrated that residue 31 of the myotoxic Asp49-PLA_2s (PrTX-III and BthTX-II) presents a different conformation when compared to the classic Asp49-PLA_2s [Fig. 6(A)] and to Lys49-PLA_2s.[61] An inspection of this region in two crystallographic structures of enzimatically-active snake venom Asp49-PLA_2s bound to calcium[92,93] and which, like BthTX-II, presents a tryptophan in position 31 of their amino acid

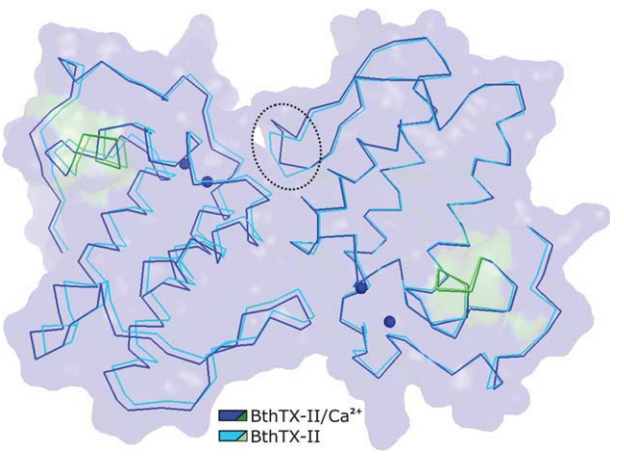

Figure 5

Superposition of apo and calcium complexed BthTX-II crystallographic structures. Regions in green indicate the calcium binding loops and the encircled area indicates the region with highest r.m.s.d. between the two structures. Blue spheres correspond to calcium ions from BthTXII/Ca^{2+} crystallographic structure. [Color figure can be viewed in the online issue, which is available at wileyonlinelibrary.com.]

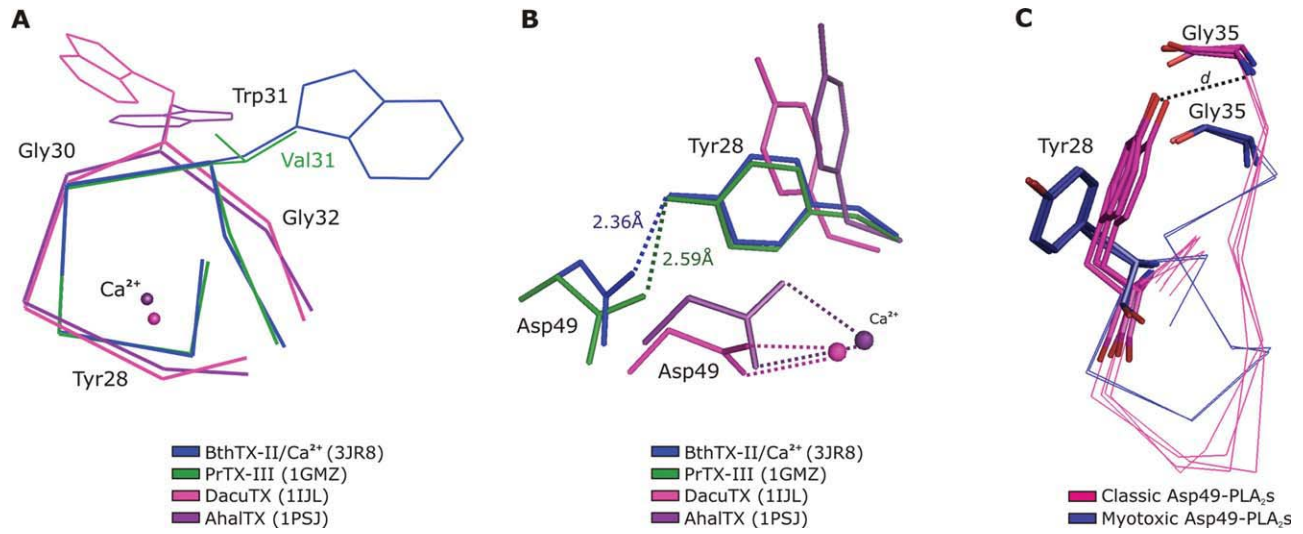

Figure 6

Inspection of the calcium-binding-loop region from some Viperidae snake venom PLA_2s. (**A**) Superposition of the calcium binding loop from two myotoxic Asp49-PLA_2s (BthTX-II/Ca^{2+} in blue and PrTX-III[62] in green) and two acidic and nonmyotoxic Asp49-PLA_2s (AhalTX[92] in purple and DacuTX[93] in pink) shows the presence of tryptophan in position 31 does not impair calcium coordination. (**B**) Tyr28 and Asp49 residues' configurations in myotoxic and nonmyotoxic Asp49-PLA_2s. Orientation of Tyr28 in myotoxic Asp49-PLA_2s leads to the establishment of a hydrogen bond between Oη from this residue and atom Oδ from Asp49, and consequently impairs Ca^{2+} coordination by both Oδ from Asp49. (**C**) Oη from Tyr28 side chain and Gly35 amino group configurations for classic Asp49-PLA_2s (magenta) and myotoxic Asp49-PLA_2s (blue) structures. Distance (*d*) between Oη of Tyr28 and the amino group of Gly35 for classic Asp49-PLA_2s is shown ($3.1 < d < 3.5$). The classic Asp49-PLA_2s are represented by AhalTX, an acidic phospholipase A_2 from *Agkistrodon halys pallas* venom (AhalTX),[92] a PLA_2 from *Daboia russelli pulchella* venom[94] and an acidic phospholipase A_2 from *Deinagkistrodon acutus* (DacuTX).[93] The myotoxic Asp49-PLA_2s (blue) are represented by BthTX-II[61] and PrTX-III.[62] [Color figure can be viewed in the online issue, which is available at wileyonlinelibrary.com.]

sequences indicates that the presence of this residue in position 31 does not impair Ca^{2+} coordination [Fig. 6(A,B)]. Interestingly, the sequence from the region 25 to 35 of the myotoxic BthTX-II is identical to the sequence of the acidic PLA_2 from the venom of *Agkistrodon halys pallas*[92] (later renamed as *Gloydius halys*; named AhalTX in Fig. 6). Therefore, the calcium binding loop distortion and its consequent inability to bind calcium ion cannot be attributed only to the presence of specific residues in the primary sequence of myotoxic Asp49-PLA_2s.

Nevertheless, two interesting features regarding the calcium binding loop distortion are observed: (i) a hydrogen bond is established between the Oδ from Asp49 and the Oη from Tyr28[61] in the myotoxic BthTX-II and PrTX-III structures whereas both Oδ atoms from Asp49 side chain are responsible for Ca^{2+} coordination in classic Asp49-PLA_2s[8,14,95] [Fig. 6(B)], and (ii) an interaction between Oη from Tyr28 and the Gly35 amino group with a conserved distance range in classic Asp49-PLA_2s ($3.1 < d < 3.5$ Å) [Fig. 6(C); Table II]. These patterns that allow a subdivision between classic and myotoxic Asp49-PLA_2s are due to the different side-chain orientation of Asp49 and residues of the calcium binding loop region [Fig. 6(B,C)].

The Tyr28-Gly35 interaction observed in classic Asp49-PLA_2s may provide structural stability for the Ca^{2+} binding loop since residues considered essential for the cofactor coordination are kept in favorable orientations when this interaction is present. On the other hand, when the distance *d* is not preserved (Fig. 6; Table II), a great distortion in the calcium-binding-loop region occurs and impairs Ca^{2+} coordination. This observation is in agreement with Zhou *et al.*[96] who proposed the absence of this interaction as being responsible for the Ca^{2+} binding loop disarrangement in Ser49-PLA_2 Ecarpholin S from *Echis carinatus sochureki* venom.

An alternative dimer may explain specific features of myotoxic Asp49-PLA_2s

Snake venom PLA_2s are capable of exerting different biological activities (e.g. catalytic, myotoxic, neurotoxic,

Table II
Distance (*d*) from Oη Atom of Tyr28 to Gly35 Amino Group in Asp49-PLA_2s Structures

	Protein (PDB identification code)	*d* (Å)
classic Asp49-PLA_2s	BthA-I-PLA_2 (1U73)[83]	3.07
	Acid-PLA_2 from *G. halys*[a] (1PSJ)[78]	3.50
	Acid-PLA_2 from *D. acutus* (1IJL)[79]	3.49
	$DPLA_2$ (1FB2)[82]	3.51
	β2-Bungarotoxin (1BUN)[84]	3.51
	Bovine pancreatic PLA_2 (1G4I)[85]	3.28
myotoxic Asp49-PLA_2s	PrTX-III (1GMZ)[62]	7.87
	BthTX-II (2OQD)[61]	7.64

[a]formerly *Agkistrodon halys pallas.*

Table III
Interfacial Area and Solvation Free Energy for BthTX-II, BthTX-II/Ca^{2+}, PrTX-III, and DacuTX Crystallographic Structures[a]

Proteins/Dimer type	Interfacial area (Å^2)	Δ^iG (kcal/mol)[b]
BthTX-II (2OQD)		
Crystallographic dimer	456.5	−2.7
Biological dimer	669.5	−13.5
BthTX-II/Ca^{2+} (3JR8)		
Crystallographic dimer	422.5	−1.5
Biological dimer	632.6	−14.5
PrTX-III (1GMZ)		
Crystallographic dimer	522.3	0.3
Biological dimer	639.9	−10.4
DacuTX (1IJL)		
Biological /crystallog. dimer	992.7	−15.6

[a]Values given by the online interactive tool PISA[93] available at the European Bioinformatics Institute server (http://www.ebi.ac.uk). Δ^iG indicates the solvation free energy gain upon formation of the interface, in kcal/mol. The value is calculated as difference in total solvation energies of isolated and interfacing structures.
[b]Negative Δ^iG corresponds to hydrophobic interfaces, or positive protein affinity. This value does not include the effect of satisfied hydrogen bonds and salt bridges across the interface. Interface area in Å^2, calculated as difference in total accessible surface areas of isolated and interfacing structures divided by two.

hypotensive, anticoagulant, bactericidal, and edema-inducing, among others). A large number of structures of these proteins has been solved, many of which present different quaternary assemblies despite possessing conserved tertiary structures.[56,61,84,86,91,97–103] Therefore, the key to understanding the mechanisms underlying their biological activities may be found by examining their oligomeric assemblies.[104]

Comparison of BthTX-II and PrTX-III structures with a dimeric Asp49-PLA_2 from *Deinagkistrodon acutus*[93] (named as DacuTX), whose structure presents a tryptophan in position 31 and Ca^{2+} coordinated by Asp49 and residues of its calcium binding loops, suggested that the cause of such distortion could be related to the oligomeric assembly adopted by myotoxic Asp49-PLA_2s toxins. As previously described, BthTX-II and PrTX-III crystallographic structures have a two-fold axis symmetry that adopts a quaternary structure resembling the Lys49-PLA_2 "conventional dimer". On the other hand, submission of these structures to PISA program[76] analyses indicated another quaternary assembly as the probable biological dimer for the myotoxins under analysis (Table III; Fig. 7) (the crystallographic structure of AhalTX was not used in this specific analysis because it is monomeric). In this suggested biological configuration, residues 31 of

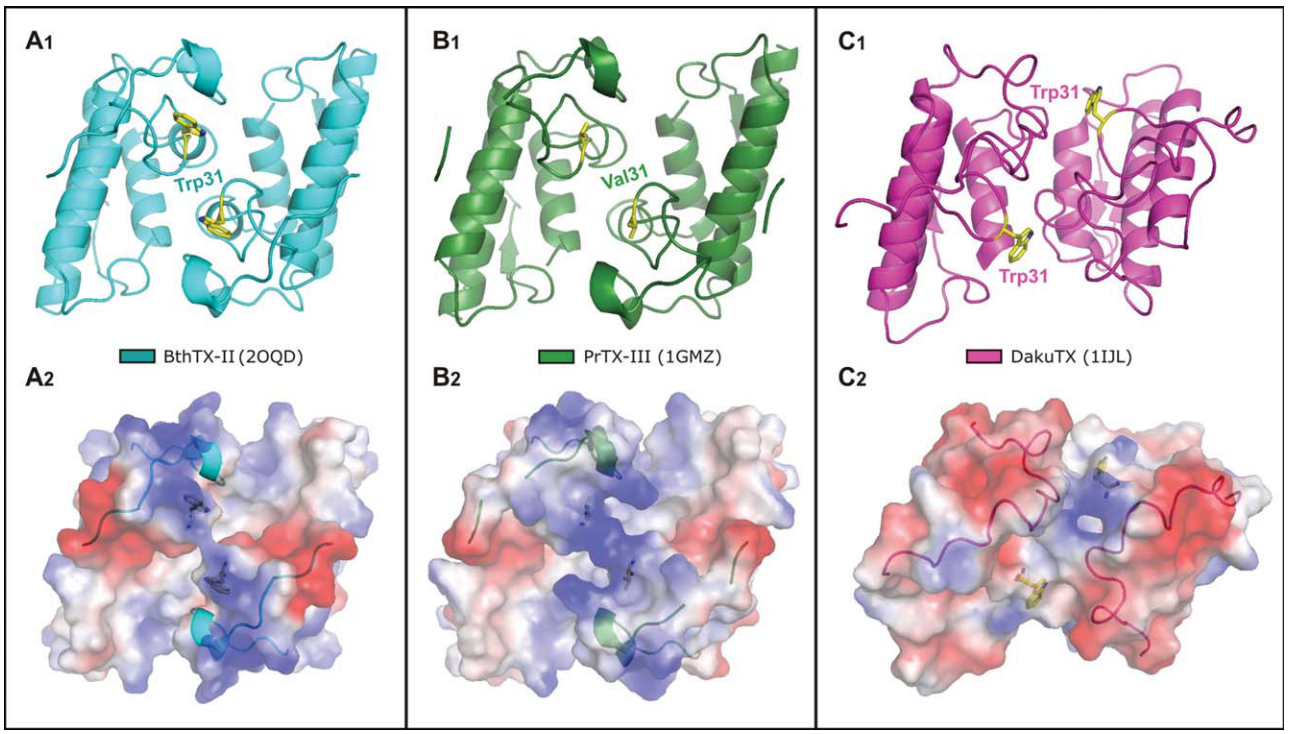

Figure 7
Biological oligomeric assemblies adopted by BthTX-II (A_1), PrTX-III (B_1), and DacuTX (C_1) apo structures. A_1 also represents BthTX-II/Ca^{2+} dimeric configuration as indicated by PISA program analyses.[76] Residues 31 are disposed side by side and towards the C-terminal region in myotoxic Asp49-PLA_2s (A_2 and B_2), establishing a direct route of communication between the calcium binding loop and the C-termini of these myotoxic proteins. A_2, B_2, and C_2 represent surface electrostatic charge distribution for the proteins under analysis. Basic surface charge distribution is observed along the C-terminal regions of the myotoxic proteins BthTX-II and PrTX-III (A_2 and B_2, respectively). The C-terminal region (amino acids 111 to 133) of BthTX-II, PrTX-III, and DacuTX shown in panels A_2, B_2, and C_2, respectively, are drawn in cartoon. [Color figure can be viewed in the online issue, which is available at wileyonlinelibrary.com.]

Table IV
Positively Charged Residues (Arginine, Lysine, and Histidine) Distribution along the C-Terminal Region[a] of svPLA$_2$s

Myotoxic PLA$_2$s[b]	Cgod2	Tgra1	Tfla1	Ooki2	MjTX-I	BthTX-I	Basp1	BthTX-II	PrTX-III
	6	7	5	6	6	7	6	7	8
Catalytic PLA$_2$s[b]	Tfla5	Bsch2	Ooki1	BthA-1	Catr1	Bery1	Apispis2	Cgod3	Pmuc1
	3	3	3	3	3	2	5	5	5

[a]Residues numbered between 111–133 in Lys49-PLA$_2$s and the ones corresponding to this sequence in Asp49-PLA$_2$s were evaluated.
[b]Protein codes can be checked in Table V.

both monomers from the myotoxic Asp49-PLA$_2$s are part of the interface and oriented towards their C-terminal region [Fig. 7(A,B)]. As a consequence of this configuration, a direct connection between their calcium binding loops and C-termini of these myotoxins is established [Fig. 7(A,B)]. Additionally, it is important to highlight that the residues 31 of myotoxic Asp49-PLA$_2$s are disposed side by side and towards their C-termini, a feature that probably conveys mechanical support for them [Fig. 7(A,B)]. Analyses of DacuTX structure shows that despite they present residues tryptophan 31 of both monomers in the interface, their calcium binding loops are not side by side and no connection between these residues and the C-termini of the protein is established [Fig 7(C)].

The C-terminal region of Lys49-PLA$_2$s has already been demonstrated to be responsible for myotoxicity expression in these proteins.[34,44,47–55] Given that the myotoxic Asp49-PLA$_2$s can be grouped into the same clade of Lys49-PLA$_2$s (Fig. 8), it is reasonable to hypothesize that their myotoxicity may also arise from their C-termini. Additionally, Francis *et al.* had already suggested that the residues between Thr112 and Pro121 from BthTX-II primary sequence are the responsible for its myotoxic activity.[30,59] Supporting these suggestions, analysis of the C-terminal region showed BthTX-II and PrTX-III present a high content of positively charged residues in their C-termini (Table IV) [Fig. 7(A,B)]. This pattern is also observed in Lys49-PLA$_2$s and is thought to be the responsible for their myotoxicity[34] (Table IV).

The hypothesis proposed above is based on a structure-function relationship. It justifies the calcium binding loop distortion in myotoxic Asp49-PLA$_2$s since BthTX-II and PrTX-III are not catalytically active and also based on the need for this distortion to stabilize their dimeric assembly and their C-termini. Additionally, in this configuration their C-termini are disposed side by side, a feature that has already been demonstrated to be important for myotoxic activity expression in Lys49-PLA$_2$s.[56]

Evolutionary inferences about snake venom phospholipases A_2 and phylogenetic relationships of myotoxic Asp49-PLA$_2$s

The results presented herein indicate that BthTX-II is able to damage myotubes but does not present catalytic activity. Interestingly, this toxin is an Asp49-PLA$_2$ and conserves the residues of the catalytic network and the ones responsible for Ca^{2+} coordination.[59,61] In order to get insights into this apparent paradox and clarify the phylogenetic relationships of BthTX-II and other myotoxic Asp49-PLA$_2$s, phylogenetic studies on snake venom PLA$_2$s from the Crotalinae subfamily were performed. Evolutional and phylogenetic studies of snake venom PLA$_2$s from the Viperidae family based on distance methods and using a few amino acid sequences had already been performed.[36,105] However, the phylogenetic relationships of myotoxic Asp49-PLA$_2$s remained unclear highlighting the importance of new studies. Herein, we present a Bayesian phylogenetic analysis for snake venom phospholipases A_2 (Fig. 8) using almost all amino acid sequences from the Crotalinae subfamily (Viperidae family) available in the NCBI databank (Table V) (only redundant sequences were discarded). Furthermore, the sequence of Gln49-PLA$_2$ from *Gloydius ussuriensis* was also included in the analysis after being manually extracted from the article.[106]

The phylogenetic tree presented here (Fig. 8) shows two main monophyletic clades (A and B) that have a common ancestor. For the first time, Asp49-PLA$_2$s are shown to be part of both clades indicating an aspartate residue occupying position 49 of the ancestor since the data of Ohno *et al.*[105] and of Wei *et al.*[36] were inconclusive about which residue occupied this position. The key difference between the Clades A and B remain on the activity exerted by proteins grouped under these branches. Proteins grouped together in Clade A present catalytic activity whereas the ones grouped in Clade B are capable of inducing local myonecrosis. The most basal sequences of Clade B are the myotoxic Asp49-PLA$_2$s, including BthTX-II (Bjar3) and PrTX-III (Bpir3). These results indicate that myotoxic Asp49-PLA$_2$s have a closer phylogenetic relationship to Lys49-PLA$_2$s than to classic Asp49-PLA$_2$s since they form a monophyletic clade with Lys49-PLA$_2$s (Fig. 8). These data are consistent with our findings for BthTX-II since this protein presents pronounced myotoxic activity but not catalysis.

The most basal sequences of Clade A (with exception of Bsch2) and all the sequences present in Clade B present a basic pI (Table V), suggesting a basic PLA$_2$ (and an Asp49 as previously shown) as the ancestor for snake venom phospholipases A_2 from the Crotalinae subfamily. On the other hand, most of the sequences of Clade A present an acidic pI (Table V), suggesting that phospholipidic activity expression is favored by this biochemical property. Interestingly, we can observe that sequences from the genera *Agkistrodon* and *Trimesurus* (Apispis2,

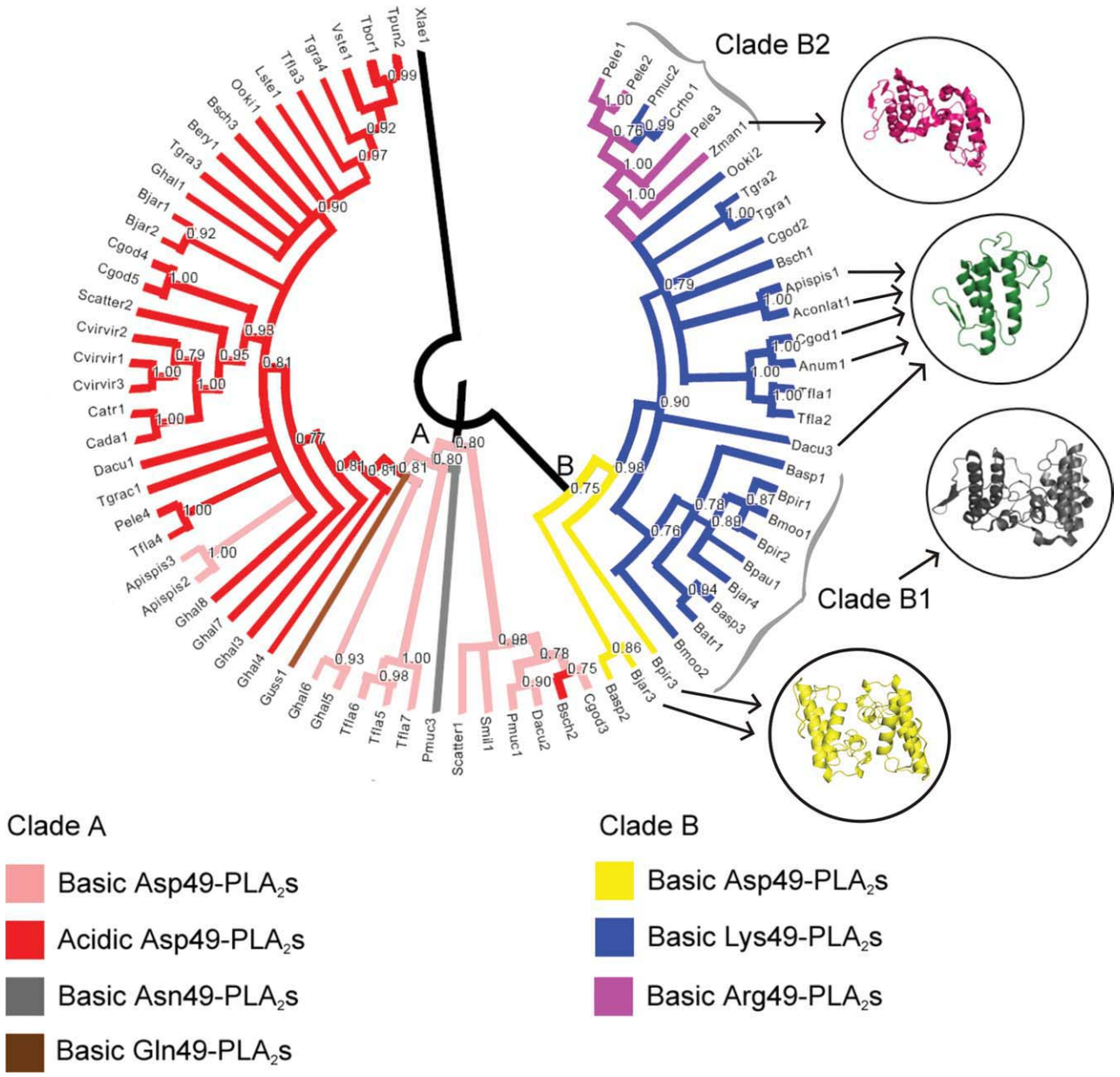

Figure 8

Phylogenetic tree of phospholipases A_2 amino acid sequences from Viperidae family (Crotalinae subfamily) snake venom. The branch color corresponds to the group to which each sequence belongs. Posterior probability values after 3,000,000 cycles are indicated in internodes. Internodes with a posterior probability value less than 0.75 were collapsed. The identification codes of the sequences are shown in Table V. Internodes with posterior probability values less than 0.75 were collapsed. Minimum *e*-value of 3.10^{-44}. Displayed oligomeric configurations are represented by apo BthTX-II (yellow), apo PrTX-I (grey), Dacu3 (green), and Zman1 (pink) structures. The biological dimer suggested by PISA[76] was used for PrTX-I and BthTX-II structures' illustrations. The representative dimeric assemblies of BthTX-II and Zman1 are the same. Proteins indicated as monomers (in green) are result of crystallographic studies and may not reflect the true biological conformation of the toxins under physiological conditions since they were crystallized in acidic pHs or in the presence of a great amount of salt (factors that can be responsible for dimer dissociation in svPLA$_2$s).

Apispis3, Tbor1 and Tpun2) (Fig. 8) experienced a reversal of their net charge that restored a basic pI. This may be a result of specific evolutional pressure on phospholipases A_2 of these two snake genera. A basic pI, on the other hand, seems to be important for expression of the myotoxic activity since all myotoxic proteins present in this phylogenetic tree possess this characteristic (Guss1, Pmuc3 and all the sequences grouped together in Clade B) (Table V) [Fig. 8(A,B)]. However, there are a few acidic Asp49-PLA$_2$s characterized as myotoxic proteins[107,108]

Table V
Identification Codes, Theoretical Isoeletric Points, NCBI, and PDB Entry Codes that Correspond to the Phospholipases A_2 from Crotalinae Subfamily present in the Phylogenetic Tree of Figure 8

	Class	Snake	Protein	Identification code	NCBI entry code	PDB entry code	Isoeletric point[a]
Clade B	**Lys49**	*Agkistrodon contortrix laticinctus*	Myotoxin	Aconlat1	1352702	1S8G/1S8H/1S8I	8.48
		Agkistrodon piscivorus piscivorus	APP-K-49	Apispis1	129478	1PPA	8.48
		Atropoides nummifer	Myotoxin II	Anum1	17433156	2AOZ	8.28
		Bothriechis schlegelii	Bsc-K49	Bsch1	25453450	-	8.61
		Bothrops asper	M1-3-3 protein	Basp3	6492260	-	8.86
		Bothrops asper	Myotoxin II	Basp1	166215047	1CLP/1Y4L	8.87
		Bothrops atrox	Myotoxin I	Batr1	40888878	-	8.48
		Bothrops jararacussu	Bothropstoxin-I (BthTX-I)	Bjar4	265051	2H8I/3CXI/3HZD/3IQ3	8.87
		Bothrops moojeni	Myotoxin II (MjTX-II)	Bmoo2	17865560	1XXS	8.61
		Bothrops moojeni	Myotoxin I (MjTX-I)	Bmoo1	17368325	-	8.61
		Bothrops pauloensis	Bnsp-7	Bpau1	239938675	1PA0	8.61
		Bothrops pirajai	Piratoxin-I (PrTX-I)	Bpir1	17433154	2Q2J/2OK9/3CYL	8.61
		Bothrops pirajai	Piratoxin-II (PrTX-II)	Bpir2	17368328	1QLL	8.72
		Calloselasma rhodostoma	G6K49	Crho1	27151658	-	8.48
		Cerrophidion godmani	Pgo-K49	Cgod2	26397687	-	8.48
		Cerrophidion godmani	Myotoxin II (GODMT-II)	Cgod1	3122600	1GOD	8.15
		Deinagkistrodon acutus	Dac-K49II	Dacu3	26397573	1MC2/1MG6	8.36
		Ovophis okinavensis	Phospholipase A_2 homolog PLA_2-03	Ooki 2	26006828	-	7.76
		Protobothrops mucrosquamatus	TMV-K49	Pmuc2	129468	-	8.48
		Trimeresurus flavoviridis	Basic protein I/II (BP-I/BP-II)	Tfla1	400717	-	8.72
		Trimeresurus flavoviridis	Basic protein II	Tfla2	222955	-	8.87
		Trimeresurus gramineus	PLA_2-VII	Tgra2	20177995	-	8.43
		Trimeresurus gramineus	PLA_2-V	Tgra1	3914265	-	8.28
	myotoxic Asp49	*Bothrops asper*	Myotoxin III	Basp2	166214965	-	8.28
		Bothrops jararacussu	Bothropstoxin-II (BthTX-II)	Bjar3	1171971	2OQD/3JR8	8.02
		Botrops pirajai	Piratoxin-III (PrTX-III)	Bpir3	17865540	1GMZ	7.87
	Arg49	*Protobothrops elegans*	Phospholipase A_2	Pele3	84578889	-	8.48
		Protobothrops elegans	Phospholipase A_2	Pele2	84578891	-	8.48
		Protobothrops elegans	Phospholipase A_2	Pele1	84578893	-	8.48
		Zhaoermia mangshanensis	Zhaoermiatoxin	Zman1	115502551	2PH4	8.61

(Continued)

Table V
(Continued)

	Class	Snake	Protein	Identification code	NCBI entry code	PDB entry code	Isoeletric point[a]
Clade A	**Classical Asp49**	*Agkistrodon piscivorus piscivorus*	APP-D-49	Apispis2	2851578	1VAP	8.15
		Bothriechis schlegelii	acidic phospholipase A_2	Bsch3	59726986	-	4.23
		Bothriechis schlegelii	N6 basic phospholipase A_2	Bsch2	38230125	-	6.74
		Bothrops erythromelas	BE-I-PLA_2	Bery1	86450426	-	4.51
		Bothrops jararacussu	BthA-I	Bjar1	25140377	1U73/1UMV/1Z76/1ZL7/ IZLB	5.21
		Bothrops jararaca	BJ-PLA_2	Bjar2	3914258	-	4.41
		Cerrophidion godmani	D1E6b phospholipase A_2	Cgod5	59727030	-	4.60
		Cerrophidion godmani	N6 basic phospholipase A_2	Cgod3	38230123	-	7.86
		Cerrophidion godmani	N1E6a phospholipase A_2	Cgod4	59727008	-	4.82
		Crotalus adamanteus	Acid Phospholipase A_2	Cada1	129507	-	4.91
		Crotalus atrox	Phospholipase A_2	Catr1	25108915	1PP2	4.47
		Crotalus viridis viridis	Acid Phospholipase A_2	Cvirvir1	28893826	-	5.21
		Crotalus viridis viridis	Acid Phospholipase A_2	Cvirvir3	28893822	-	4.76
		Crotalus viridis viridis	Acid Phospholipase A_2	Cvirvir2	28893824	-	4.47
		Deinagkistrodon acutus	Phospholipase A_2	Dacu2	97180272	-	8.16
		Deinagkistrodon acutus	Acid Phospholipase A_2 (DacuTX)	Dacu1	90265326	1IJL	4.53
		Gloydius halys	Phospholipase A_2	Ghal1	2460035	-	4.66
		Gloydius halys	Phospholipase A_2 BA2	Ghal3	27151650	-	4.80
		Gloydius halys	Phospholipase A_2 BA1	Ghal4	27151649	-	4.80
		Gloydius halys	Phospholipase A_2	Ghal7	27151651	1M8R/1M8S	4.67
		Gloydius halys[b]	Acid Phospholipase A_2 (AhalTX)[b]	Ghal8	129399	1PSJ/1BK9	4.67
		Gloydius halys	Phospholipase A_2	Ghal5	27151648	-	8.35
		Gloydius halys	B-PLA_2 phospholipase A_2	Ghal6	27151647	1B4W/1CIJ/1JIA	8.28
		Lachesis stenophrys	LSPA-1	Lste1	76363284	-	4.76
		Ovophis okinavensis	Phospholipase A_2	Ooki1	1769398	-	4.66
		Protobothrops elegans	Phospholipase A_2	Pele4	84578888	-	5.89
		Protobothrops mucrosquamatus	Trimucrotroxin	Pmuc1	26006835	-	8.02
		Sistrurus catenatus tergeminus	Phospholipase A_2	Scatter2	45934756	-	4.78
		Sistrurus catenatus tergeminus	N6b basic phospholipase A2	Scatter1	38230127	-	7.86
		Sistrurus miliarius	Phospholipase A_2	Smil1	166012664	-	7.76
		Trimeresurus borneensis	E6 acidic phospholipase A_2	Tbor1	38230145	-	5.20
		Trimeresurus flavoviridis	Phospholipase A_2	Tfla5	28202237	-	7.76
		Trimeresurus flavoviridis	TFV PL-X	Tfla7	129499	-	8.07
		Trimeresurus flavoviridis	Phospholipase A_2	Tfla3	436249	-	4.58
		Trimeresurus flavoviridis	Phospholipase A_2	Tfla4	436247	-	6.75
		Trimeresurus flavoviridis	Phospholipase A_2	Tfla6	28202238	-	7.87
		Trimeresurus gracilis	Acid Phospholipase A_2	Tgrac1	59727071	-	4.53
		Trimeresurus gramineus	PLA_2-III	Tgra3	3914270	-	4.56
		Trimeresurus gramineus	PLA_2-II	Tgra4	3914268	-	4.76
		Trimeresurus puniceus	G6D49 phospholipase A_2	Tpun2	38230137	-	5.20
		Viridovipera stejnegeri	PLA_2-V	Vste1	13959432	-	4.57
	Asn 49	*Protobothrops mucrosmatus*	TM-N49	Pmuc3	77021843	-	8.16
	Gln49	*Gloydius ussuriensis*	Gln49-PLA_2	Guss1	[c]	-	7.80
Outgroup		*Xenopus laevis*	Otoconin-22	Xlae1	385670	-	5.02

[a]Calculated by the DAMBE software.[98]
[b]formerly as *Agkistrodon halys pallas* (AhalTX).
[c]Sequence manually extracted from the article.[95]

that have not yet been entirely sequenced and hence are not present in our analysis. Although it is very difficult to determine their phylogenetic position without their complete amino acid sequences, we suspect that these sequences will be grouped in Clade A, as catalytic acidic proteins that gained myotoxic function.

As previously noted, Clade B is formed only by myotoxic proteins, most of which are Lys49-PLA_2s. Many studies have shown that the C-terminal portion of Lys49-PLA_2s is responsible for their myotoxicity expression[34,44,47] through the insertion of positively charged residues in the muscle membrane.[34] Given the large content of positively charged residues in the C-termini of myotoxic Asp49-PLA_2s and Lys49-PLA_2s (Table IV), it may be inferred that this feature was already present in the common ancestor of all sequences that form Clade B. However, an inspection of the possible quaternary assemblies exhibited by these proteins showed that they can present different oligomeric configurations, despite exerting the same biological function, as we can observe for Clades B1, B2 and for other proteins (Fig. 8). Therefore, it is possible to infer that different and specific myotoxic sites may be present among proteins that compose Clade B, although the myotoxic activity is caused by the C-terminal region. This observation is in agreement with dos Santos *et al.*[56] whose findings led to the proposal of a myotoxic site exclusive to bothropic Lys49-PLA_2s since all sequences grouped together in Clade B1 are from the *Bothrops* genus and are represented by the same oligomeric assembly.

CONCLUDING REMARKS

BthTX-II has long been known to be a bothropic snake venom compound. However, the characterization of its pharmacological properties has been misunderstood for many years. This study provides an important and novel contribution to better knowledge of this myotoxic Asp49-PLA_2. For the first time it has been shown that BthTX-II does not present catalytic activity, thus refuting the notion that all Asp49-PLA_2s are enzymes. Moreover, it has also been demonstrated that myotoxic Asp49-PLA_2s have a stronger phylogenetic relationship with Lys49-PLA_2s than with the classic Asp49-PLA_2s, as evidenced by phylogenetic analyses and by other experiments which demonstrated they do not present catalytic activity but are myotoxic, as other proteins from branch B (Fig. 8).

Recently, Bonfim *et al.* showed that BthTX-II presents a higher myotoxic effect than BthTX-I (a Lys49 PLA_2 from *Bothrops jararacussu* snake venom) and attributed the additional potency to an indirect effect related to the catalytic activity exerted by this protein.[63] On the other hand, our experiments have demonstrated that BthTX-II is able to induce practically the same level of muscle damage in the absence of calcium as the Lys49-PLA_2 BthTX-I.[89] Additionally, BthTX-II was demonstrated to cause the same level of myotoxicity at 30 min in the presence and absence of Ca^{2+} when 50 μg/mL of the toxin is tested in myotube cells [Fig. 3(C)], another piece of evidence that calcium is not required for its activity. Phylogenetic and crystallographic studies were performed and support this finding. Therefore, based on our results, it is possible to infer that Branch B of the phylogenetic tree groups only sequences of myotoxic and probably noncatalytic proteins whereas Branch A is formed by catalytic snake venom PLA_2s that can also exhibit additional pharmacological properties.

This work highlights the necessity of considering the biological quaternary assembly when functionally analyzing snake venom PLA_2s. Any clue based only on primary sequence analyses cannot be conclusive since even PLA_2s that perform common activities (e.g. myotoxicity) present different quaternary assemblies, as evidenced by analysis of oligomeric configurations exhibited by myotoxins grouped under Branch B of our phylogenetic study. Furthermore, the placement of BthTX-II in the myotoxic clade and the high content of positively charged residues along its C-terminal region indicate the need for experimental studies to prove whether this function is also exerted by residues of its C-terminal region as is already known for Lys49-PLA_2s.

In conclusion, this study provides new and strong evidences about the myotoxicity and noncatalytic activity of BthTX-II. It also supplies new insights that explain the role of Trp31, the importance of its distortion for BthTX-II activity and highlights the connection between the C-terminal and the calcium binding loop regions of BthTX-II and PrTX-III myotoxic Asp49-PLA_2s.

Atomic coordinates

The coordinates were deposited in the Protein Data Bank with identification code 3JR8.

ACKNOWLEDGMENTS

This work was supported by CARIPARO, FAPESP, CNPq, INCTTOX, and LNLS. We would like to thank Prof. Cesare Montecucco and Prof. Pedro Padilha for their support during the development of this work.

REFERENCES

1. van Deenen LLM, de Haas GH, Heemskerk CHT. Hydrolysis of synthetic mixed-acid phosphatides by phospholipase A from human pancreas. Biochim Biophys Acta 1963;67:295–304.
2. Berk PD, Stump DD. Mechanisms of cellular uptake of long chain free fatty acids. Mol Cell Biochem 1999;192:17–31.
3. Gijon MA, Leslie CC. Regulation of arachidonic acid release and cytosolic phospholipase A2 activation. J Leukoc Biol 1999;65:330–336.
4. Austin SC, Funk CD. Insight into prostaglandin, leukotriene, and other eicosanoid functions using mice with targeted gene disruptions. Prostaglandins Other Lipid Mediat 1999;58:231–252.
5. Bingham CO, III, Austen KF. Phospholipase A2 enzymes in eicosanoid generation. Proc Assoc Am Physicians 1999;111:516–524.

6. Balsinde J, Balboa MA, Dennis EA. Identification of a third pathway for arachidonic acid mobilization and prostaglandin production in activated P388D1 macrophage-like cells. J Biol Chem 2000;275:22544–22549.
7. Moolenaar WH, Kranenburg O, Postma FR, Zondag GC. Lysophosphatidic acid: G-protein signalling and cellular responses. Curr Opin Cell Biol 1997;9:168–173.
8. Arni RK, Ward RJ. Phospholipase A2—a structural review. Toxicon 1996;34:827–841.
9. Renetseder R, Dijkstra BW, Huizinga K, Kalk KH, Drenth J. Crystal-structure of bovine pancreatic phospholipase-A2 covalently inhibited by para-bromo-phenacyl-bromide. J Mol Biol 1988;200:181–188.
10. Yu BZ, Berg OG, Jain MK. The divalent cation is obligatory for the binding of ligands to the catalytic site of secreted phospholipase A2. Biochemistry 1993;32:6485–6492.
11. Six DA, Dennis EA. The expanding superfamily of phospholipase A(2) enzymes: classification and characterization. Biochim Biophys Acta 2000;1488:1–19.
12. Kudo I, Murakami M. Phospholipase A2 enzymes. Prostaglandins Other Lipid Mediat 2002;68–69:3–58.
13. White SP, Scott DL, Otwinowski Z, Gelb MH, Sigler PB. Crystal structure of cobra-venom phospholipase A2 in a complex with a transition-state analogue. Science 1990;250:1560–1563.
14. Scott DL, White SP, Otwinowski Z, Yuan W, Gelb MH, Sigler PB. Interfacial catalysis: the mechanism of phospholipase A2. Science 1990;250:1541–1546.
15. Schaloske RH, Dennis EA. The phospholipase A2 superfamily and its group numbering system. Biochim Biophys Acta 2006;1761:1246–1259.
16. Heinrikson RL, Krueger ET, Keim PS. Amino acid sequence of phospholipase A2-alpha from the venom of *Crotalus adamanteus*. A new classification of phospholipases A2 based upon structural determinants. J Biol Chem 1977;252:4913–4921.
17. Calvete JJ, Juarez P, Sanz L. Snake venomics. Strategy and applications. J Mass Spectrom 2007;42:1405–1414.
18. Andriao-Escarso SH, Soares AM, Fontes MR, Fuly AL, Correa FM, Rosa JC, Greene LJ, Giglio JR. Structural and functional characterization of an acidic platelet aggregation inhibitor and hypotensive phospholipase A(2) from Bothrops jararacussu snake venom. Biochem Pharmacol 2002;64:723–732.
19. Beers SA, Buckland AG, Koduri RS, Cho W, Gelb MH, Wilton DC. The antibacterial properties of secreted phospholipases A2: a major physiological role for the group IIA enzyme that depends on the very high pI of the enzyme to allow penetration of the bacterial cell wall. J Biol Chem 2002;277:1788–1793.
20. Bon C, Changeux JP, Jeng TW, Fraenkel-Conrat H. Postsynaptic effects of crotoxin and of its isolated subunits. Eur J Biochem 1979;99:471–481.
21. Chang CC, Lee JD, Eaker D, Fohlman J. Short communications the presynaptic neuromuscular blocking action of taipoxin. A comparison with beta-bungarotoxin and crotoxin. Toxicon 1977;15:571–576.
22. Gerrard JM, Robinson P, Narvey M, McNicol A. Increased phosphatidic acid and decreased lysophosphatidic acid in response to thrombin is associated with inhibition of platelet aggregation. Biochem Cell Biol 1993;71:432–439.
23. Condrea E, Yang CC, Rosenberg P. Lack of correlation between anticoagulant activity and phospholipid hydrolysis by snake venom phospholipases A2. Thromb Haemost 1981;45:82–85.
24. Gutiérrez JM, Lomonte B. Phospholipase A2 miotoxins from Bothrops snake venoms. In: Kini RM, editor. Phospholipases A2 Enzymes: Structure, Function, and Mechanism. Chichester: Wiley; 1997. p 321–352.
25. Lloret S, Moreno JJ. Oedema formation and degranulation of mast cells by phospholipase A2 purified from porcine pancreas and snake venoms. Toxicon 1993;31:949–956.
26. Paramo L, Lomonte B, Pizarro-Cerda J, Bengoechea JA, Gorvel JP, Moreno E. Bactericidal activity of Lys49 and Asp49 myotoxic phospholipases A2 from Bothrops asper snake venom--synthetic Lys49 myotoxin II-(115-129)-peptide identifies its bactericidal region. Eur J Biochem 1998;253:452–461.
27. Rosenberg P. Phospholipases. In: Shyer WT, Mebs D, editors. Handbook of toxinology. New York: Dekker; 1990. p 67–277.
28. Kini RM. Structure-function relationships and mechanism of anticoagulant phospholipase A2 enzymes from snake venoms. Toxicon 2005;45:1147–1161.
29. Barbosa PS, Martins AM, Havt A, Toyama DO, Evangelista JS, Ferreira DP, Joazeiro PP, Beriam LO, Toyama MH, Fonteles MC, Monteiro HS. Renal and antibacterial effects induced by myotoxin I and II isolated from Bothrops jararacussu venom. Toxicon 2005;46:376–386.
30. Francis B, Gutierrez JM, Lomonte B, Kaiser, II. Myotoxin II from Bothrops asper (Terciopelo) venom is a lysine-49 phospholipase A2. Arch Biochem Biophys 1991;284:352–359.
31. Geoghegan P, Angulo Y, Cangelosi A, Diaz M, Lomonte B. Characterization of a basic phospholipase A2-homologue myotoxin isolated from the venom of the snake Bothrops neuwiedii (yarara chica) from Argentina. Toxicon 1999;37:1735–1746.
32. Gutierrez JM, Chaves F, Gene JA, Lomonte B, Camacho Z, Schosinsky K. Myonecrosis induced in mice by a basic myotoxin isolated from the venom of the snake *Bothrops nummifer* (jumping viper) from Costa Rica. Toxicon 1989;27:735–745.
33. Gutierrez JM, Lomonte B. Phospholipase A2 myotoxins from Bothrops snake venoms. Toxicon 1995;33:1405–1424.
34. Lomonte B, Angulo Y, Calderon L. An overview of lysine-49 phospholipase A2 myotoxins from crotalid snake venoms and their structural determinants of myotoxic action. Toxicon 2003;42:885–901.
35. Mebs D, Kuch U, Coronas FIV, Batista CVF, Gumprecht A, Possani LD. Biochemical and biological activities of the venom of the Chinese pitviper Zhaoermia mangshanensis, with the complete amino acid sequence and phylogenetic analysis of a novel Arg49 phospholipase A(2) myotoxin. Toxicon 2006;47:797–811.
36. Wei JF, Wei XL, Chen QY, Huang T, Qiao LY, Wang WY, Xiong YL, He SH. N49 phospholipase A2, a unique subgroup of snake venom group II phospholipase A2. Biochim Biophys Acta 2006;1760:462–471.
37. Gutierrez JM, Lomonte B, Cerdas L. Isolation and partial characterization of a myotoxin from the venom of the snake Bothrops nummifer. Toxicon 1986;24:885–894.
38. Nishioka Sde A, Silveira PV. A clinical and epidemiologic study of 292 cases of lance-headed viper bite in a Brazilian teaching hospital. Am J Trop Med Hyg 1992;47:805–810.
39. Otero R, Gutierrez J, Beatriz Mesa M, Duque E, Rodriguez O, Luis Arango J, Gomez F, Toro A, Cano F, Maria Rodriguez L, Caro E, Martinez J, Cornejo W, Mariano Gomez L, Luis Uribe F, Cardenas S, Nunez V, Diaz A. Complications of Bothrops, Porthidium, and Bothriechis snakebites in Colombia. A clinical and epidemiological study of 39 cases attended in a university hospital. Toxicon 2002;40:1107–1114.
40. Gutierrez JM, Theakston RD, Warrell DA. Confronting the neglected problem of snake bite envenoming: the need for a global partnership. PLoS Med 2006;3:e150.
41. Cardoso JL, Fan HW, Franca FO, Jorge MT, Leite RP, Nishioka SA, Avila A, Sano-Martins IS, Tomy SC, Santoro ML, Chudzinski AM, Castro SCB, Kamiguti AS, Kelen EMA, Hirata MH, Mirandola RMS, Theakston RDG, Warrell DA. Randomized comparative trial of three antivenoms in the treatment of envenoming by lance-headed vipers (Bothrops jararaca) in Sao Paulo, Brazil. Q J Med 1993;86:315–325.
42. Milani R, Jorge MT, DeCampos FPF, Martins FP, Bousso A,REFAU>Cardoso JLC,Ribeiro LA, Fan HW, Franca FOS, SanoMartins IS, Cardoso D, Fernandez IDOF, Fernandes JC, Aldred VL, Sandoval MP, Puorto G, Theakston RDG, Warrell DA. Snake bites by the jararacucu (Bothrops jararacussu): clinicopatho-

logical studies of 29 proven cases in Sao Paulo State, Brazil. QJM-Mon J Assoc Physicians 1997;90:323–334.
43. Lomonte B, Leon G, Angulo Y, Rucavado A, Nunez V. Neutralization of Bothrops asper venom by antibodies, natural products and synthetic drugs: contributions to understanding snakebite envenomings and their treatment. Toxicon 2009;54:1012–1028.
44. Ward RJ, Chioato L, de Oliveira AH, Ruller R, Sa JM. Active-site mutagenesis of a Lys49-phospholipase A2: biological and membrane-disrupting activities in the absence of catalysis. Biochem J 2002;362 (Part 1):89–96.
45. Maraganore JM, Merutka G, Cho W, Welches W, Kezdy FJ, Heinrikson RL. A new class of phospholipases A2 with lysine in place of aspartate 49. Functional consequences for calcium and substrate binding. J Biol Chem 1984;259:13839–13843.
46. dos Santos JI, Fernandes CA, Magro AJ, Fontes MR. The intriguing phospholipases A2 homologues: relevant structural features on myotoxicity and catalytic inactivity. Protein Pept Lett 2009;16:887–893.
47. Chioato L, de Oliveira AHC, Ruller R, Sa JM, Ward RJ. Distinct sites for myotoxic and membrane-damaging activities in the C-terminal region of a Lys(49)-phospholipase A(2). Biochem J 2002;366:971–976.
48. Chioato L, Aragao EA, Ferreira TL, de Medeiros AI, Faccioli LH, Ward RJ. Mapping of the structural determinants of artificial and biological membrane damaging activities of a Lys49 phospholipase A(2) by scanning alanine mutagenesis. Biochim Et Biophys Acta-Biomemb 2007;1768:1247–1257.
49. Nunez CE, Angulo Y, Lomonte B. Identification of the myotoxic site of the Lys49 phospholipase A(2) from Agkistrodon piscivorus piscivorus snake venom: synthetic C-terminal peptides from Lys49, but not from Asp49 myotoxins, exert membrane-damaging activities. Toxicon 2001;39:1587–1594.
50. Ward RJ, Alves AR, Ruggiero Neto J, Arni RK, Casari G. A SequenceSpace analysis of Lys49 phopholipases A2: clues towards identification of residues involved in a novel mechanism of membrane damage and in myotoxicity. Protein Eng 1998;11:285–294.
51. Cintra-Francischinelli M, Pizzo P, Angulo Y, Gutierrez JM, Montecucco C, Lomonte B. The C-terminal region of a Lys49 myotoxin mediates Ca2+ influx in C2C12 myotubes. Toxicon 2010;55:590–596.
52. Calderon L, Lomonte B. Immunochemical characterization and role in toxic activities of region 115-129 of myotoxin II, a Lys49 phospholipase A2 from Bothrops asper snake venom. Arch Biochem Biophys 1998;358:343–350.
53. Calderon L, Lomonte B. Inhibition of the myotoxic activity of Bothrops asper myotoxin II in mice by immunization with its synthetic 13-mer peptide 115-129. Toxicon 1999;37:683–687.
54. Lomonte B, Pizarro-Cerda J, Angulo Y, Gorvel JP, Moreno E. Tyr-->Trp-substituted peptide 115-129 of a Lys49 phospholipase A(2) expresses enhanced membrane-damaging activities and reproduces its in vivo myotoxic effect. Biochim Biophys Acta 1999;1461:19–26.
55. Lomonte B, Angulo Y, Santamaria C. Comparative study of synthetic peptides corresponding to region 115-129 in Lys49 myotoxic phospholipases A2 from snake venoms. Toxicon 2003;42:307–312.
56. dos Santos JI, Soares AM, Fontes MR. Comparative structural studies on Lys49-phospholipases A(2) from Bothrops genus reveal their myotoxic site. J Struct Biol 2009;167:106–116.
57. Homsi-Brandeburgo MI, Queiroz LS, Santo-Neto H, Rodrigues-Simioni L, Giglio JR. Fractionation of Bothrops jararacussu snake venom: partial chemical characterization and biological activity of bothropstoxin. Toxicon 1988;26:615–627.
58. Gutierrez JM, Nunez J, Diaz C, Cintra AC, Homsi-Brandeburgo MI, Giglio JR. Skeletal muscle degeneration and regeneration after injection of bothropstoxin-II, a phospholipase A2 isolated from the venom of the snake Bothrops jararacussu. Exp Mol Pathol 1991;55:217–229.
59. Pereira MF, Novello JC, Cintra AC, Giglio JR, Landucci ET, Oliveira B, Marangoni S. The amino acid sequence of bothropstoxin-II, an Asp-49 myotoxin from Bothrops jararacussu (Jararacucu) venom with low phospholipase A2 activity. J Protein Chem 1998;17:381–386.
60. Toyama MH, Costa PD, Novello JC, de Oliveira B, Giglio JR, da Cruz-Hofling MA, Marangoni S. Purification and amino acid sequence of MP-III 4R D49 phospholipase A2 from Bothrops pirajai snake venom, a toxin with moderate PLA2 and anticoagulant activities and high myotoxic activity. J Protein Chem 1999;18:371–378.
61. Correa LC, Marchi-Salvador DP, Cintra AC, Sampaio SV, Soares AM, Fontes MR. Crystal structure of a myotoxic Asp49-phospholipase A2 with low catalytic activity: insights into Ca2+-independent catalytic mechanism. Biochim Biophys Acta 2008;1784:591–599.
62. Rigden DJ, Hwa LW, Marangoni S, Toyama MH, Polikarpov I. The structure of the D49 phospholipase A2 piratoxin III from Bothrops pirajai reveals unprecedented structural displacement of the calcium-binding loop: possible relationship to cooperative substrate binding. Acta Crystallogr D Biol Crystallogr 2003;59 (Part 2):255–262.
63. Bonfim VL, de Carvalho DD, Ponce-Soto LA, Kassab BH, Marangoni S. Toxicity of phospholipases A2 D49 (6-1 and 6-2) and K49 (Bj-VII) from Bothrops jararacussu venom. Cell Biol Toxicol 2009;25:523–532.
64. Fuly AL, Soares AM, Marcussi S, Giglio JR, Guimaraes JA. Signal transduction pathways involved in the platelet aggregation induced by a D-49 phospholipase A2 isolated from Bothrops jararacussu snake venom. Biochimie 2004;86:731–739.
65. McPherson A. Introduction to macromolecular crystallography. Hoboken: Wiley-Liss; 2003. 237 p.
66. Otwinowski Z, Minor W. Processing of X-ray diffraction data collected in oscillation mode. Macromol Crystallogr A 1997;276:307–326.
67. Brunger AT. Free R value: a novel statistical quantity for assessing the accuracy of crystal structures. Nature 1992;355:472–475.
68. Murshudov GN, Vagin AA, Dodson EJ. Refinement of macromolecular structures by the maximum-likelihood method. Acta Crystallogr D Biol Crystallogr 1997;53 (Part 3):240–255.
69. Emsley P, Cowtan K. Coot: model-building tools for molecular graphics. Acta Crystallogr D Biol Crystallogr 2004;60(Part 12, Part 1):2126–2132.
70. Brunger AT, Adams PD, Clore GM, DeLano WL, Gros P, Grosse-Kunstleve RW, Jiang JS, Kuszewski J, Nilges M, Pannu NS, Read RJ, Rice LM, Simonson T, Warren GL. Crystallography & NMR system: a new software suite for macromolecular structure determination. Acta Crystallogr Sect D-Biol Crystallogr 1998;54:905–921.
71. Harding MM. Geometry of metal-ligand interactions in proteins. Acta Crystallogr D Biol Crystallogr 2001;57 (Part 3):401–411.
72. Harding MM. The geometry of metal-ligand interactions relevant to proteins. II. Angles at the metal atom, additional weak metal-donor interactions. Acta Crystallogr D Biol Crystallogr 2000;56 (Part 7):857–867.
73. Fraústo da Silva JJR, Willians RJP. The Biological Chemistry of the Elements—The Inorganic Chemistry of Life. Oxford University Press: Oxford; 1991. 561 p.
74. Laskowski RA, Macarthur MW, Moss DS, Thornton JM. Procheck—a program to check the stereochemical quality of protein structures. J Appl Crystallogr 1993;26:283–291.
75. Jones TA, Bergdoll M, Kjeldgaard M. O: a macromolecule modeling environment. In: Bugg C, Ealick SE, editors. Crystallographic and Modeling Methods in Molecular Design. New York: Springer-Verlag; 1990. p 189–195.
76. Krissinel E, Henrick K. Inference of macromolecular assemblies from crystalline state. J Mol Biol 2007;372:774–797.
77. DeLano WL. The PyMOL molecular graphics system. San Carlos, CA: DeLano Scientific LLC; 2002.
78. Schwartz AS, Pachter L. Multiple alignment by sequence annealing. Bioinformatics 2007;23:e24–e29.

79. Huelsenbeck JP, Ronquist F. MRBAYES: Bayesian inference of phylogenetic trees. Bioinformatics 2001;17:754–755.
80. Maddison WP, Maddison DR. Mesquite: a modular system for evolutionary analysis. Version 2.72. 2009. Available at: http://mesquiteproject.org/mesquite2.72/mesquite/mesquite.html.
81. Kaiser, II, Gutierrez JM, Plummer D, Aird SD, Odell GV. The amino acid sequence of a myotoxic phospholipase from the venom of Bothrops asper. Arch Biochem Biophys 1990;278:319–325.
82. Lomonte B, Gutierrez JM. A new muscle damaging toxin, myotoxin II, from the venom of the snake Bothrops asper (terciopelo). Toxicon 1989;27:725–733.
83. Cintra AC, Marangoni S, Oliveira B, Giglio JR. Bothropstoxin-I: amino acid sequence and function. J Protein Chem 1993;12:57–64.
84. Arni RK, Ward RJ, Gutierrez JM, Tulinsky A. Structure of a calcium-independent phospholipase-like myotoxic protein from Bothrops asper venom. Acta Crystallogr D Biol Crystallogr 1995;51 (Part 3):311–317.
85. Soares AM, Rodrigues VM, Homsi-Brandeburgo MI, Toyama MH, Lombardi FR, Arni RK, Giglio JR. A rapid procedure for the isolation of the Lys-49 myotoxin II from Bothrops moojeni (caissaca) venom: biochemical characterization, crystallization, myotoxic and edematogenic activity. Toxicon 1998;36:503–514.
86. Watanabe L, Soares AM, Ward RJ, Fontes MRM, Arni RK. Structural insights for fatty acid binding in a Lys49-phospholipase A(2): crystal structure of myotoxin II from Bothrops molojeni complexed with stearic acid. Biochimie 2005;87:161–167.
87. Angulo Y, Gutierrez JM, Soares AM, Cho W, Lomonte B. Myotoxic and cytolytic activities of dimeric Lys49 phospholipase A(2) homologues are reduced, but not abolished, by a pH-induced dissociation. Toxicon 2005;46:291–296.
88. Murakami MT, Vicoti MM, Abrego JRB, Lourenzoni MR, Cintra ACO, Arruda EZ, Tomaz MA, Melo PA, Arni RK. Interfacial surface charge and free accessibility to the PLA(2)-active site-like region are essential requirements for the activity of Lys49 PLA(2) homologues. Toxicon 2007;49:378–387.
89. Cintra-Francischinelli M, Pizzo P, Rodrigues-Simioni L, Ponce-Soto LA, Rossetto O, Lomonte B, Gutierrez JM, Pozzan T, Montecucco C. Calcium imaging of muscle cells treated with snake myotoxins reveals toxin synergism and presence of acceptors. Cell Mol Life Sci 2009;66:1718–1728.
90. Matthews BW. Solvent content of protein crystals. J Mol Biol 1968;33:491–497.
91. Murakami MT, Arruda EZ, Melo PA, Martinez AB, Calil-Elias S, Tomaz MA, Lomonte B, Gutierrez JM, Arni RK. Inhibition of myotoxic activity of Bothrops asper myotoxin II by the anti-trypanosomal drug surarnin. J Mol Biol 2005;350:416–426.
92. Wang XQ, Yang J, Gui LL, Lin ZJ, Chen YC, Zhou YC. Crystal structure of an acidic phospholipase A2 from the venom of Agkistrodon halys pallas at 2.0 A resolution. J Mol Biol 1996;255:669–676.
93. Gu L, Zhang H, Song S, Zhou Y, Lin Z. Structure of an acidic phospholipase A2 from the venom of Deinagkistrodon acutus. Acta Crystallogr D Biol Crystallogr 2002;58 (Part 1):104–110.
94. Chandra V, Kaur P, Jasti J, Betzel C, Singh TP. Regulation of catalytic function by molecular association: structure of phospholipase A2 from Daboia russelli pulchella (DPLA2) at 1.9 A resolution. Acta Crystallogr D Biol Crystallogr 2001;57 (Part 12): 1793–1798.
95. Scott DL, Otwinowski Z, Gelb MH, Sigler PB. Crystal structure of bee-venom phospholipase A2 in a complex with a transition-state analogue. Science 1990;250:1563–1566.
96. Zhou X, Tan TC, Valiyaveettil S, Go ML, Kini RM, Velazquez-Campoy A, Sivaraman J. Structural characterization of myotoxic ecarpholin S from Echis carinatus venom. Biophys J 2008;95:3366–3380.
97. Arni RK, Fontes MR, Barberato C, Gutierrez JM, Diaz C, Ward RJ. Crystal structure of myotoxin II, a monomeric Lys49-phospholipase A2 homologue isolated from the venom of *Cerrophidion* (Bothrops) *godmani*. Arch Biochem Biophys 1999;366:177–182.
98. Magro AJ, Murakami MT, Marcussi S, Soares AM, Arni RK, Fontes MR. Crystal structure of an acidic platelet aggregation inhibitor and hypotensive phospholipase A2 in the monomeric and dimeric states: insights into its oligomeric state. Biochem Biophys Res Commun 2004;323:24–31.
99. Magro AJ, Soares AM, Giglio JR, Fontes MR. Crystal structures of BnSP-7 and BnSP-6, two Lys49-phospholipases A(2): quaternary structure and inhibition mechanism insights. Biochem Biophys Res Commun 2003;311:713–720.
100. Marchi-Salvador DP, Correa LC, Magro AJ, Oliveira CZ, Soares AM, Fontes MR. Insights into the role of oligomeric state on the biological activities of crotoxin: crystal structure of a tetrameric phospholipase A2 formed by two isoforms of crotoxin B from Crotalus durissus terrificus venom. Proteins 2008;72:883–891.
101. Murakami MT, Melo CC, Angulo Y, Lomonte B, Arni RK. Structure of myotoxin II, a catalytically inactive Lys49 phospholipase A(2) homologue from Atropoides nummifer venom. Acta Crystallogr Sect F: Struct Biol Cryst Commun 2006;62:423–426.
102. Murakami MT, Gabdoulkhakov A, Genov N, Cintra ACO, Betzel C, Arni RK. Insights into metal ion binding in phospholipases A(2): ultra high-resolution crystal structures of an acidic phospholipase A(2) in the Ca2+ free and bound states. Biochimie 2006;88:543–549.
103. Marchi-Salvador DP, Fernandes CA, Silveira LB, Soares AM, Fontes MR. Crystal structure of a phospholipase A(2) homologue complexed with p-bromophenacyl bromide reveals important structural changes associated with the inhibition of myotoxic activity. Biochim Biophys Acta 2009;1794:1583–1590.
104. Magro AJ, Fernandes CA, dos Santos JI, Fontes MR. Influence of quaternary conformation on the biological activities of the Asp49-phospholipases A2s from snake venoms. Protein Pept Lett 2009;16:852–859.
105. Ohno M, Chijiwa T, Oda-Ueda N, Ogawa T, Hattori S. Molecular evolution of myotoxic phospholipases A2 from snake venom. Toxicon 2003;42:841–854.
106. Chang Y, Li Y, Bao Y, An L. Neurotoxic activity of Gln49 phospholipase A(2) from Gloydius ussuriensis snake venom. J Appl Toxicol 2007;27:447–452.
107. Rodrigues RS, Izidoro LFM, Teixeira SS, Silveira LB, Hamaguchi A, Homsi-Brandeburgo MI, Selistre-de-Araujo HS, Giglio JR, Fuly AL, Soares AM, Rodrigues VM. Isolation and functional characterization of a new myotoxic acidic phospholipase A(2) from Bothrops pauloensis snake venom. Toxicon 2007;50:153–165.
108. Santos-Filho NA, Silveira LB, Oliveira CZ, Bernardes CP, Menaldo DL, Fuly AL, Arantes EC, Sampaio SV, Mamede CC, Beletti ME, de Oliveira F, Soares AM. A new acidic myotoxic, anti-platelet and prostaglandin I2 inductor phospholipase A2 isolated from Bothrops moojeni snake venom. Toxicon 2008;52:908–917.